organics

MDPI

Review

Advances in Organic Materials for Next-Generation Optoelectronics: Potential and Challenges

Ghazi Aman Nowsherwan *,†, Qasim Ali †, Umar Farooq Ali, Muhammad Ahmad, Mohsin Khan and Syed Sajjad Hussain

Centre of Excellence in Solid State Physics, University of the Punjab, Lahore 54590, Pakistan
* Correspondence: ghaziaman.pu@gmail.com
† These authors contributed equally to this work.

Abstract: This review provides a comprehensive overview of recent advancements in the synthesis, properties, and applications of organic materials in the optoelectronics sector. The study emphasizes the critical role of organic materials in the development of state-of-the-art optoelectronic devices such as organic solar cells, organic thin-film transistors, and OLEDs. The review further examines the structure, operational principles, and performance metrics of organic optoelectronic devices. Organic materials have emerged as promising candidates due to their low-cost production and potential for large-area or flexible substrate applications. Additionally, this review highlights the physical mechanisms governing the optoelectronic properties of high-performance organic materials, particularly photoinduced processes relevant to charge carrier photogeneration. It discusses the unique benefits of organic materials over traditional inorganic materials, including their light weight, simple processing, and flexibility. The report delves into the challenges related to stability, scalability, and performance, while highlighting the wide range of electronic properties exhibited by organic materials, which are critical for their performances in optoelectronic devices. Furthermore, it addresses the need for further research and development in this field to achieve consistent performance across different types of devices.

Keywords: organic material; organic solar cell; OLED; phototransistor; photodetector

Citation: Nowsherwan, G.A.; Ali, Q.; Ali, U.F.; Ahmad, M.; Khan, M.; Hussain, S.S. Advances in Organic Materials for Next-Generation Optoelectronics: Potential and Challenges. *Organics* **2024**, *5*, 520–560. https://doi.org/10.3390/org5040028

Academic Editor: Wim Dehaen

Received: 30 September 2024
Revised: 22 October 2024
Accepted: 7 November 2024
Published: 11 November 2024

1. Introduction

Organic materials are primarily classified as compounds that contain carbon–hydrogen bonds. The ability to form intricate molecular structures, flexibility, and decreased density are some of the unique characteristics of organic materials compared with inorganic ones [1,2]. Many applications, including those in electronics and health, are enabled by these qualities [2,3]. Organic materials possess properties that make them particularly appropriate for specific applications because they can be produced in a multitude of ways [4,5]. Certain organic molecules, when utilized as semiconductors, have the added benefit of being lightweight and flexible, much like inorganic materials like silicon [6,7]. The greater likelihood of inorganic materials' chemical and thermal stability in harsh circumstances, on the other hand, makes them a desirable option for applications requiring toughness and resilience.

Carbon-based structures are important in organic materials, particularly in energy applications and flexible electronics. They have unique properties that allow for innovative design and functionality; they are essential to modern technology. Certain characteristics set the organic materials used in semiconductor devices apart from traditional inorganic semiconductors, and because organic semiconductors are composed of molecules based on carbon, a wide variety of structural configurations are possible. Owing to their adaptability, electronic characteristics can be customized for certain uses [8]. It is simpler to design a range of organic electronic devices because organic materials may be doped to create N-

and P-type semiconductors that function similarly to their inorganic counterparts. Charge-transfer organic conductors demonstrate remarkably high electrical conductivities, which are influenced by their molecular arrangements and phase transitions [9,10]. These materials exhibit electrical anisotropy, which may be used in cutting-edge electronic applications to improve the efficiency of devices such as organic field-effect transistors. Combining organic materials with inorganic elements, such as hybrid organic–inorganic perovskites, enhances the stability and efficiency of optoelectronic devices, thereby addressing the common limitations of organic semiconductors [11]. Figure 1 provides an overview of the unique properties of organic materials relevant to their use in optoelectronics and electronic applications. It highlights physical, chemical, structural, mechanical, optical, electrical, thermal, and photoluminescence characteristics, such as density, chemical stability, molecular alignment, flexibility, absorption coefficient, conductivity, thermal properties, and emission behavior.

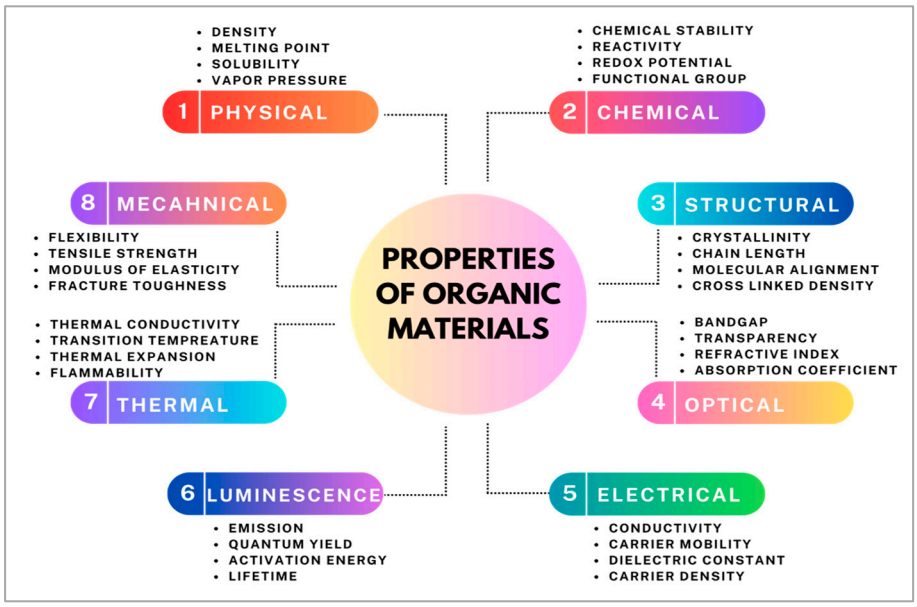

Figure 1. Diagrammatic representation of various properties of organic materials.

Carbon-based materials, such as conductive polymers and small-molecule semiconductors, enable the creation of lightweight and flexible electronic components, diverging from traditional rigid materials [12]. Techniques such as polymerization and vapor deposition enhance the integration of these materials into wearable devices, thereby promoting innovations such as skin-like interfaces [13]. The concept of super-structured carbons allows for precisely engineered materials that can be tailored for specific applications, thereby enhancing the performance of energy storage and conversion devices [14]. Activated carbon materials exhibit structural flexibility, adapting their properties based on the adsorption of different organic molecules, which can be leveraged for sensing applications [15]. Optoelectronics has improved dramatically with the discovery of organic conducting materials and electroluminescence, opening new possibilities for devices such as solar cells and OLEDs. One of the most significant discoveries is the creation of luminous organic radicals, which improve light emission capabilities by using 100% exciton efficiency owing to their special spin configurations [16]. Furthermore, the production of various organic materials has been made possible by the synthesis of π-conjugated systems via transition-metal-catalyzed oxidative coupling, which has removed earlier restrictions on material design [17]. Furthermore, advances in stretchable and flexible organic optoelectronic devices have expanded their potential use in consumer electronics and wearable technologies [18]. Research on conjugated polymers and graphene has improved optoelectronic device efficiency [19].

The use of organic materials in optoelectronic devices has attracted considerable attention owing to their unique properties and potential applications. Figure 2 displays

a number of optoelectronic applications of organic materials and polymers. The use of organic light-emitting diodes (OLEDs) is an excellent example of how organic materials are revolutionizing optoelectronics. Using organic molecules or polymers, OLEDs produce light in response to an electric current. The advantages of these materials, including flexibility, light weight, and low processing temperature, make them suitable for various display and lighting applications [20–22]. Phosphorescent transition-metal complexes have recently made significant advancements in OLED performance and efficiency. Similarly, organic materials play a major role in the development of photodetectors and phototransistors [23]. These devices, which convert light into electrical information, are essential for biological sensing, imaging, and optical communication. Among the benefits of organic photodetectors are their high photogeneration yield, adaptability in substrate construction, and effective light absorption over a broad range [24]. Technological advances, such as perovskite/organic-semiconductor vertical heterojunctions, have enabled the construction of ultrasensitive broadband phototransistors with remarkable detectivity and responsivity [25,26]. Organic solar cells (OSCs) represent a significant additional use for organic materials in optoelectronics. These solar cells convert sunlight into electricity by using organic chemicals or polymers. The advantages of OSCs are their large-area manufacturing capability, mechanical flexibility, and low manufacturing cost. Current research has focused on improving the stability and efficiency of OSCs using materials derived from biomass and advanced light control techniques [22,23,27]. Combining both organic and inorganic components, hybrid perovskites are a unique class of materials developed for optoelectronic applications. Adjustable bandgaps, excellent charge-transfer properties, and ease of manufacturing characterize these materials. Although research is currently being conducted to address stability difficulties, they have proven to function very well in photodetectors, light-emitting diodes, and solar cells [25–27].

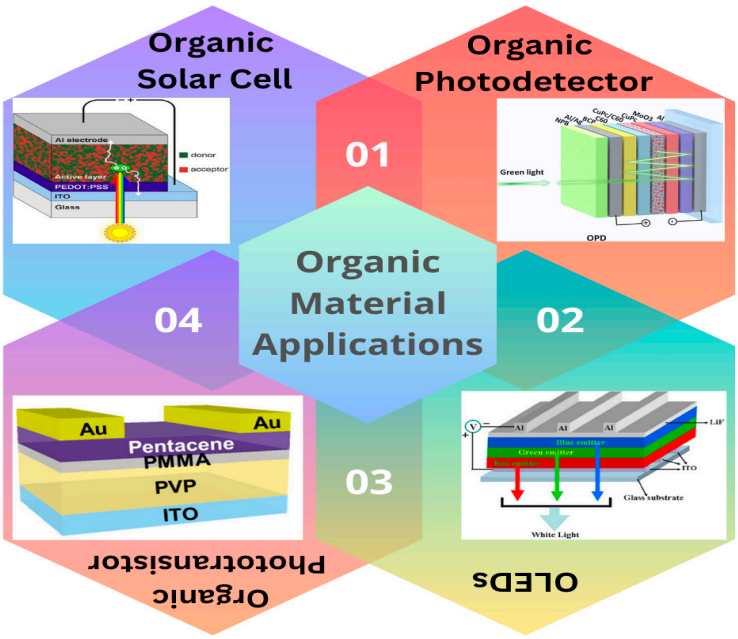

Figure 2. Illustration of various optoelectronic applications employing organic materials.

Organic semiconductors are ideal for use in conformal devices, such as flexible screens, wearable electronics, and other devices that require little weight and flexibility. Roll-to-roll manufacturing techniques, for example, are appropriate for manufacturing organic thin-film transistors (OTFTs) on flexible substrates such as polyethylene terephthalate (PET) and poly(imide) [28]. The stiffness of conventional silicon-based electronics, which are sometimes heavy and fragile, contrasts sharply with this flexibility. Compared with silicon-based technologies, organic compounds also provide better processability. Solution-based methods, which are often easier and less expensive to process than high-temperature

and high-vacuum procedures required for silicon, can be used to handle them. This covers procedures such as printing, spin-coating, and other solution-based deposition processes [29,30]. Organic electronics are even more ecologically friendly when non-toxic and safe solvents are used. In general, the fabrication of organic electronics is less expensive than that of silicon equivalents. Overall, a reduction in production costs is facilitated by the use of affordable, flexible substrates and low-temperature processing [10]. New developments in the synthesis and design of organic semiconductors have resulted in materials with high charge-carrier mobilities that are on par with or even higher than those of amorphous silicon [31].

Stability, scalability, and performance are only a few of the problems facing the synthesis and use of organic materials today [32–35]. Chemical stability is a major problem because materials such as metal–organic frameworks (MOFs) tend to break down under acidic, basic, or aqueous conditions; nevertheless, solutions such as the use of particular ligands have been investigated to increase resilience. Another issue is mechanical stability during operation, where pressure-induced modifications to MOFs' characteristics necessitate the use of sophisticated computational models for improvement. Economic feasibility and scalability continue to be major obstacles, as large-scale sustained synthetic processes are essential for practical applications. Moreover, organic materials frequently find it difficult to continue performing in challenging situations, underscoring the necessity for materials that can continue to operate and remain stable under difficult circumstances.

The goal of this study was to provide a comprehensive overview of the most recent advancements in the synthesis, properties, and applications of organic materials in the optoelectronics sector. The process flow outlined in this evaluation is illustrated in Figure 3. In addition to discussing the challenges related to stability, scalability, and performance, this review will focus on the unique benefits that organic materials possess over traditional inorganic materials, such as their light weight, simple processing, and flexibility. With an emphasis on the critical role of organic materials in the development of state-of-the-art optoelectronic devices such as organic solar cells, organic thin-film transistors, and OLEDs, this study seeks to provide an overview of the current research conditions. Possible future paths to improve the stability and functionality of these devices in real-world applications are also discussed. This research was motivated by the rapidly growing field of organic optoelectronics, which has attracted significant attention owing to the potential and versatility of organic materials in modern technology. This review seeks to bridge the knowledge gap by offering a comprehensive analysis of the techniques utilized to create organic materials, their integration into optoelectronic devices, and the potential for their use in the future for large-scale, sustainable applications in industries such as flexible electronics, energy harvesting, and wearable technology.

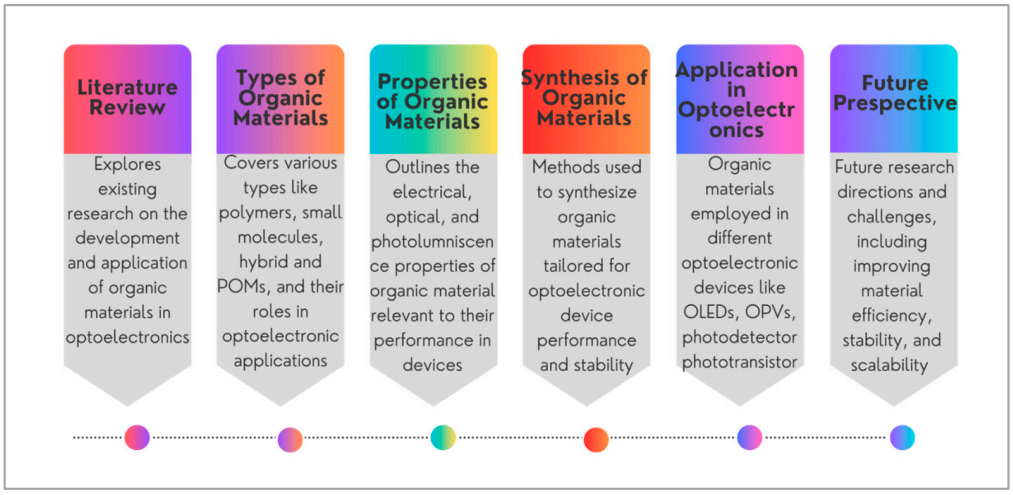

Figure 3. Process flow diagram of key stages of the review.

2. Types of Organic Materials Used in Optoelectronic Devices

Organic materials, such as conjugated polymers and small molecules, play a critical role in optoelectronic devices due to their tunable electronic and optical properties. These materials are often shared between applications, such as organic solar cells (OSCs) and organic light-emitting diodes (OLEDs), because their performance metrics, such as charge mobility, light absorption, and emission, are relevant across a broad spectrum of technologies. By understanding their behavior in one device, such as an OLED, we can apply similar principles to other technologies, including OSCs, thereby justifying a cross-application analysis of these materials.

Organic materials are currently used in the manufacture of a wide range of optoelectronic devices, including solar cells, photodetectors, OLEDs, and phototransistors. These materials have benefits such as flexibility, low cost, and room temperature processing. Below are the key types of organic materials used in these devices along with examples and their applications. Table 1 summarizes the key insights, features, and applications of organic materials.

Table 1. Summary of key materials used in organic optoelectronic devices.

Material Type	Key Materials	Features	Chemical Formula	Application	Usage	Insights
Conjugated Polymers and Small Molecules	Poly(3-hexylthiophene) (P3HT)	High charge mobility, flexibility, solution-processable	$(C_{10}H_{14}S)n$	Solar cells, Photodetectors	Light absorption, Charge transport	Common in organic photovoltaics (OPVs)
	Poly[2-methoxy-5-(2-ethylhexyloxy)-1,4-phenylene vinylene] (MEH-PPV)	High efficiency, photostability	$C_{22}H_{30}O_2$	OLEDs	Emission layer in OLEDs, Charge transport	Exhibits photoluminescence
	Pentacene	High carrier mobility	$C_{22}H_{14}$	Phototransistors, Solar cells	Organic semiconductors	Frequently used in OFETs
	Fullerene (C60)	Electron acceptor, high electron mobility	C60	Solar cells, Photodetectors	Electron acceptor in OPVs	Synergizes with conjugated polymers
Organic–Inorganic Hybrid Perovskites	Methylammonium Lead Iodide ($MAPbI_3$)	High absorption, tunable bandgap	$CH_3NH_3Pb_3$	Solar cells, Photodetectors	Light absorption, Charge transport	Exhibits rapid efficiency improvements
	Formamidinium Lead Iodide ($FAPbI_3$)	Narrow bandgap, good thermal stability	$CH(NH_2)2PbI_3$	Solar cells	Light absorption	More thermally stable than $MAPbI_3$
	Cesium Lead Bromide ($CsPbBr_3$)	Wide bandgap, high photoluminescence	$CsPbBr_3$	Photodetectors, LEDs	Light absorption, Emission	Inorganic perovskite with good stability
	Mixed-halide Perovskites ($MAPbI_3$-xClx)	Tunable properties, long carrier diffusion length	$CH_3NH_3Pb_3$-xClx	Solar cells, Photodetectors, LEDs	Enhanced optoelectronic properties	Known for stability in different environments
Thermally Activated Delayed Fluorescence (TADF) Materials	4CzIPN	High efficiency, long exciton lifetime	$C_{50}H_{40}N_4O_2$	OLEDs	Emission layer	Enables efficient OLEDs due to delayed fluorescence
	2CzPN	Efficient exciton utilization	$C_{36}H_{26}N_4O$	OLEDs	Emission layer	Low non-radiative losses

Table 1. *Cont.*

Material Type	Key Materials	Features	Chemical Formula	Application	Usage	Insights
Thermally Activated Delayed Fluorescence (TADF) Materials	DMAC-DPS	High quantum yield, tunable emission	$C_{30}H_{30}N_2S_2$	OLEDs	Emission layer, Electrolumines-cence	Exhibits delayed fluorescence
	t-BuCz-BN	High efficiency in OLED applications	$C_{36}H_{43}BN_4$	OLEDs	Charge transport and emission	TADF material enabling low-voltage OLEDs
Charge-Transfer Complexes	Tetrathiafulvalene (TTF)	High electrical conductivity, donor molecule	$C_6H_4S_4$	Photodetectors, Phototransis-tors	Charge transport, Conductivity	Common in organic electronics
	Tetracyanoquino-dimethane (TCNQ)	High electron affinity, acceptor molecule	$C_{12}H_4N_4$	Phototransistors, Solar cells	Electron transport	Used in charge-transfer complexes
	Donor–Acceptor Complexes (e.g., TTF-TCNQ)	Efficient charge separation	-	Photodetectors, Phototransis-tors	Charge transfer	Shows promising electronic properties
	Fullerene Charge-Transfer Complexes (C60 derivatives)	High electron mobility, efficient exciton dissociation	C60 derivatives	Solar cells, Photodetectors	Electron transport and charge separation	Synergizes with various donor materials
Polyoxometalates (POMs)	Phosphomolybdic Acid (PMA)	Strong oxidative properties, catalytic activity	$H_3PMo_{12}O_{40}$	Solar Cells, Photodetectors	Electron transport, Catalysis	Often used in hybrid devices
	Tungstosilicic Acid (TSA)	Excellent proton conductor, stable in humid conditions	$H_4[SiW_{12}O_{40}]$	Solar Cells, Photodetectors	Electron transport, Catalysis	Suitable for energy storage applications
	Vanadium-substituted POMs	Tunable redox properties, catalytic activity	$[PMo_{12}O_{40}]^{3-}$, $[PW_{12}O_{40}]^{3-}$	Solar Cells, Photodetectors	Electron transport	Widely used in energy conver-sion devices
	Silicotungstic Acid (STA)	High stability, redox-active	$H_4[SiW_{12}O_{40}]$	Photodetectors, Solar Cells, OLEDs	Electron transport, Catalysis	Employed in hybrid devices and OLEDs

2.1. Conjugated Polymers and Small Molecules

Conjugated polymers and small molecules are widely used in organic solar cells (OSCs), organic light-emitting diodes (OLEDs), and organic field-effect transistors (OFETs) owing to their excellent charge transport properties and tunable electronic characteristics. Key materials (bridged dithienyl) and related structures, benzodithiophene (BDT)-based polymers, Zn-Salphen-containing polymers, p-π conjugated polyelectrolytes, and p-π conjugated polyelectrolytes) include various conjugated systems that enhance the performance of optoelectronic applications. These materials exhibit low bandgaps and high stabilities, making them suitable as active components in optoelectronic devices [36]. BDT is a prominent building block owing to its symmetric structure, which facilitates excellent charge transport in devices [37]. Zn-Salphen-containing polymers demonstrate a unique aggregation behavior, enhancing their optoelectronic properties [38]. OSCs and OLEDs are only two examples of devices that benefit from the use of small molecules such as p-π conjugated polyelectrolytes as interlayer materials because they increase efficiency [39]. Figure 4 illustrates the structural formulae of several conjugated organic polymers and molecules employed in various optoelectronic applications. Further research and development in this field is necessary because despite the apparent promise of these materials, there are still problems with achieving consistent performance across different types of devices.

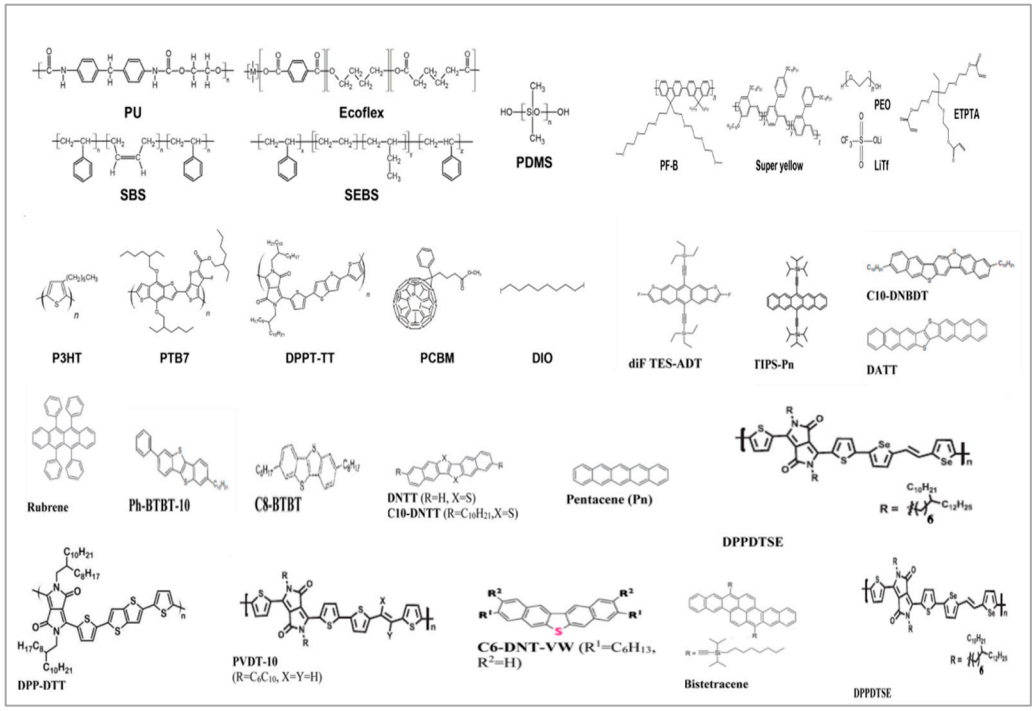

Figure 4. Structural representation of conjugated polymers and molecules in optoelectronic applications.

2.2. Organic–Inorganic Hybrid Perovskites

The unique properties of organic–inorganic hybrid perovskites (HOIPs), such as their high efficiency, tunable bandgaps, and good charge-transfer capabilities, make them essential for the development of optoelectronic devices. Significant materials in this discipline include metal halides, organic semiconductors, and two-dimensional (2D) materials, each of which offers distinct advantages for device performance. For solar cells and LEDs, hailde perovskites (ABX_3) are ideal owing to their exceptional photovoltaic properties. They have variable optical qualities owing to their different structural makeups [40,41]. Charge-transfer stability and efficiency are improved when organic semiconductors are included in perovskite frameworks, which is important for applications in LEDs and photodetectors [42]. Due to their unique heterointerface properties, 2D organic materials such as graphene and transition metal dichalcogenides combined with perovskites further improve device stability and efficiency [41]. These materials appear promising; however, problems with stability and ion migration remain significant barriers to their practical application [42]. Future studies should focus on addressing these limitations to fully fulfill the potential of hybrid perovskites in optoelectronics.

2.3. Thermally Activated Delayed Fluorescence (TADF) Materials

Organic thermally activated delayed fluorescence (TADF) materials play a crucial role in optimizing the optoelectronic device efficiency, particularly in organic light-emitting diodes (OLEDs). Various electron acceptors and performance-enhancing ligands are key materials. Amide-Based Acceptors have been demonstrated to improve efficiency and stability when they switch from carbonyl to amide units (O=C–N). An external quantum efficiency (EQEmax) of 26.0% and photoluminescence quantum yields of up to 99% have been achieved using new TADF compounds based on benzoyl and carbazoline in OLEDs [43]. Transition metal complexes, which are common on Earth, are becoming increasingly well known for their effectiveness and sustainability. These materials utilize various ligands to improve TADF properties, making them suitable for diverse applications beyond OLEDs [44]. Chiral TADF materials have been developed to fabricate intrinsically axial chiral Mult resonance TADF materials, achieving high photoluminescence quan-

tum yields (90%/91%) and external quantum efficiencies of 30.1% in circularly polarized OLEDs [45].

2.4. Charge-Transfer Complexes

Organic charge-transfer complexes (CTCs) are essential for the development of optoelectronic devices. Several electron donors and acceptors that improve the device performance through specific chemical interactions are essential components of these complexes. The majority of electron donors are carbazole-based substances, which exhibit modified optical characteristics when combined with acceptors such as 7,7,8,8-tetracyanoquinodimethane (TCNQ) [46]. The acceptor materials are Tetrathiafulvalene (TTF) combined with TCNQ, which has historically demonstrated metallic-like conductivity, marking a significant milestone in organic optoelectronics [47]. In organic photovoltaic (OPV) devices, optimization of donor–acceptor interfaces is essential for efficient charge separation and transport, with materials such as polyvinyl carbazole (PVK) being widely utilized [48]. The emphasis on CTCs is encouraging; however, obstacles such as synthesis difficulty and cost will likely prevent them from being widely used in optoelectronic devices.

2.5. Polyoxometalates (POMs)

Owing to their special qualities, including outstanding stability and adjustable electrical characteristics, polyoxometalates (POMs) are becoming important materials in optoelectronic devices. They serve several purposes, but two of the most important ones are hole transporting layers (HTLs) and anode interlayers (AILs), which significantly enhance device performance. Owing to their superior hole-collection capabilities, potassium-neutral counterions (POMs), such as NH^{4+}, K^{+}, and Na^{+}, are valuable HTLs. For example, POM-NH4 in organic solar cells (OSCs) demonstrated a power conversion efficiency of 18.0% [49]. Conjugated polyelectrolytes mutually doped with POMs exhibit enhanced p-doping capabilities. This leads to a high work function and lower energy barrier for HTLs, which improves the efficiency of OSCs and OLEDs [50]. Owing to their high work functions and superior conductivities, Dawson-type POMs are effective AILs. Devices that made use of these POMs showed a 17.8% power conversion efficiency as well as lower turn-on voltages [51]. On the other hand, although POMs have potential, there are still issues with maximizing their integration into commercial devices, especially with regard to cost-effectiveness and scalability.

3. Electronic, Optical, and Photoluminescence Properties of Organic Material Used in Optoelectronic Devices

The adjustable characteristics, flexibility, and low manufacturing cost of organic materials and polymers have attracted considerable interest in optoelectronics [9,52]. Excitons or bound electron–hole pairs are produced by light exposure in these materials and are essential for converting light into electrical or luminescent energy [53]. The molecular structure and electrical characteristics of the polymer have a significant impact on the efficiency of exciton formation, diffusion, and dissociation. Regarding optoelectronic and photonic applications, Table 2 presents the distinct qualities of these materials and underlines their applicability. These devices include organic field-effect transistors (OFETs), organic photovoltaics (OPVs), organic photodetectors (OPDs), and organic light-emitting diodes (OLEDs), depending on these materials [54].

Table 2. Summary of electronic, optical, and photoluminescence properties of some organic materials.

Material Type	Key Materials	Electronic Properties	Optical Properties	Photoluminescence Properties
Conjugated Polymers and Small Molecules	**Poly(3-hexylthiophene) (P3HT)**	High hole mobility (~0.1 cm^2/Vs), bandgap ~1.9 eV, low electron affinity	Absorption in visible range (400–650 nm), strong absorption coefficient	Photoluminescence peak at ~650 nm, high quantum efficiency
	Pentacene	High carrier mobility (~1 cm^2/Vs), low bandgap (1.9 eV), p-type semiconductor	Strong absorption near 700 nm, long-range exciton diffusion	Weak photoluminescence, low quantum yield, exciton lifetime of ~1 ns
	Fullerene (C_{60})	High electron mobility (~0.1 cm^2/Vs), efficient electron acceptor	Broad absorption spectrum (200–500 nm), high light-harvesting efficiency	Weak photoluminescence, low yield, short exciton lifetime
	MEH-PPV	Moderate hole mobility (~10^{-4} cm^2/Vs), bandgap ~2.1 eV	Absorption in the visible range (~400–600 nm)	Photoluminescence peak at ~580 nm, high quantum yield
	TIPS-Pentacene	High mobility (~0.4 cm^2/Vs), solution-processable, low bandgap	Strong absorption near 650–700 nm	Weak photoluminescence, good exciton diffusion
Organic–Inorganic Hybrid Perovskites	**Methylammonium Lead Iodide ($MAPbI_3$)**	High charge carrier mobility (~20 cm^2/Vs), tunable bandgap (1.5 eV), low recombination rate	Strong absorption across visible and near-IR range (400–800 nm), long carrier diffusion length	Strong photoluminescence at ~760 nm, high quantum yield, lifetime ~100 ns
	Cesium Lead Bromide ($CsPbBr_3$)	Moderate charge mobility (~5 cm^2/Vs), wide bandgap (~2.3 eV), good thermal stability	Absorption in UV–visible range (350–550 nm), high absorption coefficient	Strong photoluminescence at ~520 nm, high PL quantum yield (>90%)
	Formamidinium Lead Iodide ($FAPbI_3$)	High stability, low trap state density, tunable bandgap (~1.48 eV)	Strong absorption in visible region (400–800 nm)	Photoluminescence at ~780 nm, long exciton lifetime
	Mixed-Halide Perovskites ($MAPbBr_3$-xIx)	High carrier mobility, tunable bandgap (1.6–2.3 eV), low recombination	Tunable absorption (visible and near-IR), enhanced stability	Photoluminescence peak tunable from 550 to 760 nm
Thermally Activated Delayed Fluorescence (TADF) Materials	**4CzIPN**	Long exciton lifetime, efficient singlet-to-triplet conversion, high triplet energy	Strong absorption in the UV region (300–400 nm), visible emission (~500–600 nm)	Photoluminescence peak at ~520 nm, delayed fluorescence lifetime (~100 µs)
	DMAC-DPS	Efficient exciton utilization, high electron mobility	Strong absorption in UV–visible region (350–450 nm), efficient blue emission	Photoluminescence peak at ~460 nm, delayed fluorescence, high PL quantum yield
	t-BuCz-BN	High efficiency in OLEDs, good thermal stability	Absorption in the UV–visible region, visible emission (~550–600 nm)	Delayed fluorescence, photoluminescence at ~580 nm
	2CzPN	High electron mobility, efficient singlet–triplet transition	Absorption in UV–visible region (~350–400 nm), efficient blue emission	Delayed photoluminescence at ~450–500 nm
Charge-Transfer Complexes	**Tetrathiafulvalene (TTF)**	High electrical conductivity (~1 S/cm), low ionization potential (~6.8 eV)	Moderate absorption in the visible region (~350–600 nm)	Weak photoluminescence, efficient charge separation, low exciton recombination
	Tetracyanoquinodimethane (TCNQ)	High electron affinity (~4.8 eV), p-type organic semiconductor	Strong absorption near 400 nm, narrow optical bandgap (~2 eV)	Weak photoluminescence, low quantum yield
	TTF-TCNQ Complex	High charge-transfer efficiency, donor–acceptor system	Broad absorption in UV–visible range (~300–600 nm)	No significant photoluminescence, efficient charge transfer
	C_{60}-TTF Complex	High electron mobility, efficient charge separation	Absorbs in visible range, strong light absorption	Weak photoluminescence, good charge recombination
Polyoxometalates (POMs)	**Phosphomolybdic Acid (PMA)**	High redox activity, moderate electron mobility (~0.01 cm^2/Vs)	Absorption in UV–visible range (~200–450 nm), strong optical density	Low photoluminescence, strong redox-induced quenching
	Silicotungstic Acid (STA)	High stability, redox-active, wide bandgap (~4 eV)	Strong UV absorption (200–400 nm), good optical transparency	Low photoluminescence, used as electron acceptor in hybrid devices
	Vanadium-substituted POMs	High electron mobility, strong catalytic properties	Absorption in UV–visible (~300–450 nm), moderate optical density	Low photoluminescence, good charge separation
	Tungstosilicic Acid (TSA)	Good thermal stability, moderate conductivity, strong redox	Strong absorption in UV (~200–400 nm), high optical density	Low photoluminescence, strong redox-active material

Key properties of organic materials, such as charge carrier mobility, light absorption, and photoluminescence, are foundational for their performances in a variety of optoelectronic applications. For example, high charge mobility is essential for both OSCs to improve charge extraction and OLEDs to enhance light emission efficiency. Additionally, light absorption characteristics are critical for solar cell applications, while emission properties are vital for OLEDs. By exploring these shared properties across devices, we gain more holistic insights into how these materials can be optimized for diverse optoelectronic applications.

3.1. Electronic Properties of Organic Materials Employed in Optoelectronic Devices

The electrical properties of organic materials and polymers are mostly controlled by the conjugated π-electron systems present in their molecular framework [55]. The lowest unoccupied molecular orbital (LUMO) and highest occupied molecular orbital (HOMO) are two energy levels found in organic semiconductors. An important aspect in defining a material's electronic properties is its bandgap, which is determined by the energy difference between its HOMO and LUMO levels [56]. Visible light optoelectronics can benefit from the use of organic materials due to their tunable bandgaps, which typically range from 1.5 to 3 eV [57]. This tunability is achieved by modifying the molecular structure, such as varying the length of the conjugated system, adding electron-donating or withdrawing groups, or utilizing copolymers. For instance, larger bandgaps are preferable in OLEDs for achieving specific emission colors, while narrower bandgaps are more suitable for OPVs to capture a broader spectrum of solar radiation. In contrast to the band transport observed in inorganic semiconductors, such as silicon, charge transfer in organic semiconductors is typically facilitated by hopping processes, where electrons or holes move between localized states. The transport mechanisms in organic materials, especially polymers, are critical for the operation of devices like organic solar cells and light-emitting diodes.

A key difference between organic and inorganic materials lies in charge mobility. Organic semiconductors often have lower charge mobilities, typically ranging from 10^{-6} to 10^{-1} cm^2/Vs, which can limit the performance of devices like organic field-effect transistors (OFETs) and organic photovoltaic cells (OPVs) when compared with inorganic devices like silicon-based transistors, which exhibit much higher mobilities, often exceeding 100 cm^2/Vs. This difference results in faster switching times and higher efficiencies in inorganic devices. However, organic materials offer a distinct advantage in their tunability. The bandgap in organic semiconductors can be easily engineered for specific optoelectronic applications, such as optimizing light emission in OLEDs or enhancing solar energy absorption in OPVs. In contrast, inorganic semiconductors require more complex doping processes to achieve similar tunability. Despite inorganic devices generally outperforming organic ones in terms of charge mobility and stability, organic materials offer notable benefits. Their low-cost, flexible, and solution-processable natures make them advantageous for applications where mechanical flexibility, large-area production, and environmental sustainability are key. Thus, while organic materials may fall short in certain performance metrics, they provide unique opportunities in the development of next-generation, low-cost, and flexible optoelectronic devices, offering potential for innovations that inorganic materials alone cannot easily achieve.

In the highly ordered or crystalline regions of polymers, charge carriers can move more freely, akin to electrons in a conventional semiconductor band structure. The mobility μ in this regime can be significantly higher than that in hopping transport and is influenced by the presence of phonons and impurities. In disordered polymers, charge carriers typically move by hopping between localized states [58,59]. Energy is transferred non-radiatively from a donor molecule to an acceptor molecule through dipole–dipole interactions, as shown in Figure 5c. This process occurs when the donor, initially in an excited electronic state, transfers energy to the acceptor, causing the acceptor to become excited. Energy transfer occurs without the emission of a photon and relies on the proximity of the two molecules, typically within the range of 1–10 nm.

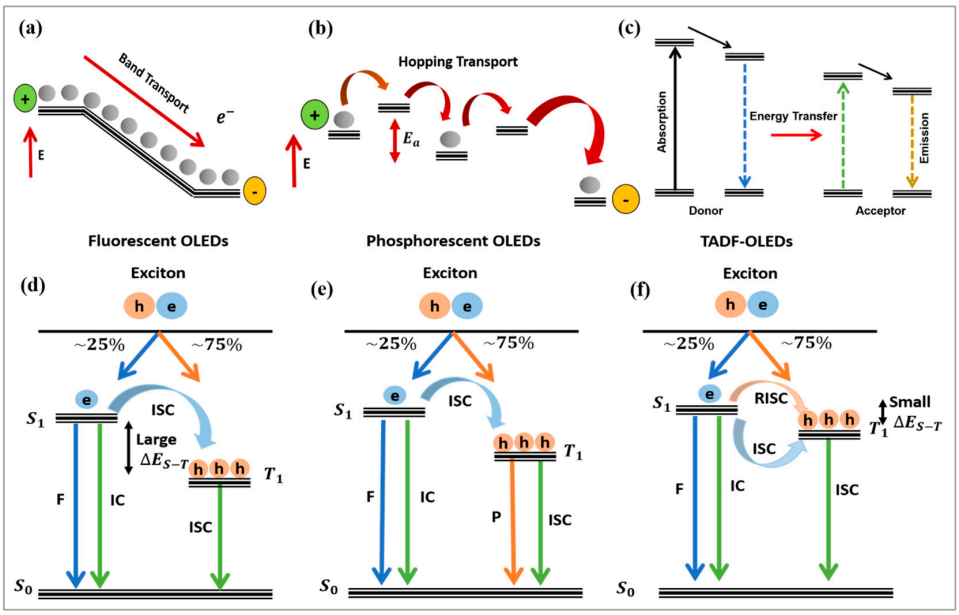

Figure 5. Diagrammatic depictions of (**a**) charge transport resembling ballistic bands and (**b**) charge transport via hopping mechanism. (**c**) The mechanism of Förster resonance energy transfer (FRET), operational principles of (**d**) fluorescence, (**e**) phosphorescence, and (**f**) thermally activated delayed fluorescence.

The impact of charge traps on charge transport depends on the trap density and depth, that is, the energy difference between the trap level and band edge. In field-effect transistors (FETs), shallow traps (with depths on the order of several kBT) reduce the mobility and manifest as a gradual turn-on of the transistor. Deep traps (with depths much greater than kBT) can shift the threshold voltage without significantly affecting mobility or subthreshold behavior. Akin to interface trap density in a conventional semiconductor-based device structure, the presence of interface trap density can be detrimental to the overall performance of the device [60]. The mobility of charge carriers in organic materials is generally lower than that of their inorganic counterparts, with typical values ranging from 10^{-6} to 10^{-1} cm^2/Vs, and is influenced by factors such as molecular packing, crystallinity, and the presence of traps or defects [61]. In OFETs, a high mobility is essential for efficient charge injection and transport. Strategies to improve mobility include optimizing the molecular packing through thermal annealing or solvent engineering and designing polymers with high degrees of planarity and π–π stacking interactions [62].

The organic materials listed Table 2 exhibit a wide range of electronic properties that are critical for their performance in optoelectronic devices, such as OLEDs, solar cells, and photodetectors. Conjugated polymers such as P3HT and pentacene offer high hole mobilities (up to ~1 cm^2/Vs) and low bandgaps (~1.9 eV), making them effective in devices where efficient charge transport is essential. Hybrid perovskites, such as $MAPbI_3$ and $CsPbBr_3$, provide excellent charge mobility (up to 20 cm^2/Vs) and tunable bandgaps (1.5–2.3 eV), with the added advantage of low recombination rates, which is key for improving device efficiency. TADF materials, such as 4CzIPN, are engineered for long exciton lifetimes and efficient singlet-to-triplet conversion, thereby enhancing the energy efficiency of devices such as OLEDs. Charge-transfer complexes, such as TTF-TCNQ, focus on efficient charge transfer between donor and acceptor molecules, improving conductivity, while polyoxometalates (POMs), such as PMA and STA, exhibit redox activity and moderate electron mobility.

3.2. Optical Properties of Organic Materials Employed in Optoelectronic Devices

Optical properties such as absorption and emission are central to the operation of optoelectronic devices. These properties are directly linked to the electronic structure and

bandgap of the organic materials. Organic semiconductors predominantly absorb light through π–π * transitions in the conjugated structure. The absorption spectra of these materials can be adjusted through chemical changes, such as changing the conjugation length or adding substituents that change the electronic structure [63].

Since excitons, which are electronic excitations, are coupled to the vibrational modes of polymer molecules, the resulting optical absorption spectra frequently display complex patterns [64]. Benzene rings exhibit C–C stretching and C–H wagging, as examples of these vibrational modes. The absorption properties are strongly influenced by the interactions between these modes. A polymer molecule changes from its ground state to its excited state when it absorbs photons. This process is not merely an electronic transition, but also involves vibrational excitations. The Franck–Condon principle, which asserts that the strength of an absorption line is proportional to the overlap integral of the vibrational wavefunctions of the ground and excited states, quantifies the coupling between electronic and vibrational states. The absorption spectrum of a polymer typically features a series of peaks corresponding to transitions involving different vibrational modes [65]. These peaks provided insights into the vibronic structure of the polymer. The position and intensity of these peaks can be used to infer the coupling strength between the electronic states and specific vibrational modes as well as the nature of the vibrational modes.

In OPVs, the absorption spectrum is critical to determine the range of sunlight that can be harvested. Materials with broad absorption spectra are desirable for maximizing the photogenerated charge carriers. In addition, the absorption coefficient of organic materials is relatively high, allowing the fabrication of thin-film devices with efficient light absorption. The refractive index of organic materials is another important optical property that affects the design of optoelectronic devices. The refractive index contrast between the organic layers and adjacent materials affects the outcoupling efficiency of light in OLEDs. Organic materials can exhibit optical anisotropy owing to their molecular orientation, which is particularly relevant in devices where polarization effects are important [66].

Compared with conventional semiconductors like silicon, which exhibit predictable optical absorption primarily in the visible and near-infrared regions, organic materials offer tunable absorption properties across the UV, visible, and near-infrared (NIR) spectra. For instance, conjugated polymers such as P3HT have strong absorption in the visible range (~400–650 nm), while fullerene (C_{60}) displays broad absorption from the UV to the visible range, making them particularly suitable for applications in solar cells and photodetectors. Hybrid perovskites like $MAPbI_3$ and $CsPbBr_3$ demonstrate robust absorption across the visible spectrum (400–800 nm) with high optical density, enhancing their light-harvesting capabilities. Additionally, TADF materials such as DMAC-DPS absorb light in the UV–visible range and provide efficient blue emission, which is essential for color displays in OLEDs. Charge-transfer complexes like TTF absorb moderately in the visible region (350–600 nm), while polyoxometalates (POMs) such as STA and PMA exhibit strong absorption in the UV–visible range (200–450 nm), making them valuable for photodetector applications. This tunability and versatility in absorption characteristics position organic materials as competitive alternatives to conventional semiconductors, particularly in applications requiring flexibility and adaptability.

3.3. Photoluminescence Properties of Organic Materials

When an organic material or polymer absorbs a photon, it undergoes various relaxation processes and returns to its ground state. These processes can be broadly categorized into radiative and non-radiative pathways [67]. Non-radiative relaxation involves the dissipation of energy through mechanisms that do not emit light, including energy dissipation such as heat, collisions, and molecular conformational changes [68]. Energy dissipation occurs as heat when excess energy is transferred to the surrounding lattice or medium, resulting in thermal vibrations [69,70]. Collisions involve interactions with other molecules, which transfer energy and facilitate relaxation. Molecular conformational changes occur when the polymer undergoes structural rearrangement, releasing energy without photon

emission. These processes compete with the radiative pathways and can significantly affect the efficiency of light emission in polymers. Radiative relaxation involves the emission of photons, which contributes to the visible light output of the material. As shown in Figure 5d–f, the main radiative processes in organic materials include fluorescence, phosphorescence, and delayed fluorescence, each of which involves the emission of light from excited states.

When organic materials absorb light, excitons (bound electron–hole pairs) are generated. In contrast to inorganic semiconductors, where excitons are often weakly bound (Wannier–Mott excitons), organic materials typically form strongly bound Frenkel excitons because of their low dielectric constants [71]. These excitons can decay radiatively, emitting light during the process, which is the basis of the photoluminescence observed in OLEDs. The emission color of OLEDs is directly related to the energy gap between the excited and ground states. The emission wavelength can be tuned across the visible spectrum by modifying the molecular structure. For instance, blue, green, and red emitters have been developed for full-color displays. High quantum yields are desirable to achieve bright and efficient OLEDs. However, not all excitons contribute to light emission; some may undergo non-radiative decay, reducing the overall efficiency. Strategies to improve quantum yield include the use of materials with high photoluminescence efficiency, engineering the molecular environment to reduce non-radiative pathways, and incorporating phosphorescent or thermally activated delayed fluorescence (TADF) emitters that can harvest both singlet and triplet excitons for light emission [72].

The photoluminescence (PL) properties of organic materials are essential for their performance in light-emitting devices such as OLEDs and for sensing applications. Conjugated polymers such as MEH-PPV display high quantum efficiency and photoluminescence peaks in the visible spectrum (~580 nm), which are suitable for light-emitting applications. Hybrid perovskites, particularly $MAPbI_3$, exhibit strong photoluminescence at approximately 760 nm with high quantum yields and long exciton lifetimes (~100 ns), making them suitable for efficient light emission in LEDs. TADF materials excel in photoluminescence, with materials such as 4CzIPN showing delayed fluorescence (~520 nm) with lifetimes in the microsecond range, thus enhancing the energy efficiency of OLEDs. Charge-transfer complexes and POMs generally exhibit weak photoluminescence owing to efficient charge separation and redox activity, respectively, which is useful for applications that require charge transfer but not light emission, such as photodetectors.

In contrast to conventional semiconductors, which typically exhibit well-defined photoluminescence properties due to their stable band structures and effective radiative recombination processes, organic materials present unique advantages and challenges. For instance, the strong binding of Frenkel excitons in organic semiconductors leads to efficient light emission, particularly in devices like OLEDs, where the emission color can be easily tuned through molecular design. This tunability is a significant advantage over inorganic materials, which often require complex doping or structural modifications to achieve similar results. Additionally, the incorporation of advanced emitters such as phosphorescent and TADF materials allows organic devices to utilize both singlet and triplet excitons, enhancing overall efficiency and brightness. However, the propensity for non-radiative decay in organic materials can limit performance, necessitating careful engineering of molecular environments to maximize quantum yield. This contrasts with conventional semiconductors, where higher charge mobilities and lower non-radiative losses often lead to superior device performance in terms of efficiency and stability. Thus, while organic materials may exhibit lower intrinsic mobility and stability, their unique photoluminescence properties and design flexibility present compelling opportunities for innovative optoelectronic applications. Table 2 provides a deeper insight into the properties of the materials used in optoelectronic applications, such as OLEDs, solar cells, and photodetectors.

4. Deposition and Synthesis of Organic Materials

The deposition and synthesis of organic materials for optoelectronic devices can be achieved using both the bottom-up and top-down methods. The bottom-up approach involves building materials at the molecular or atomic level, typically via chemical synthesis or self-assembly techniques. This method allows precise control over the structure and properties of the material, making it ideal for creating high-quality organic semiconductors and functional layers. Conversely, the top-down approach begins with bulk materials that are then processed into desired shapes or structures. Although it may not offer the same level of control as bottom-up methods, it is effective for creating large-area devices and integrating organic materials into existing semiconductor technologies. Figures 6–8 illustrate the selective top-down and bottom-up approaches for the preparation of organic materials used in optoelectronic applications. Table 3 provides a detailed comparison between bottom-up and top-down deposition techniques.

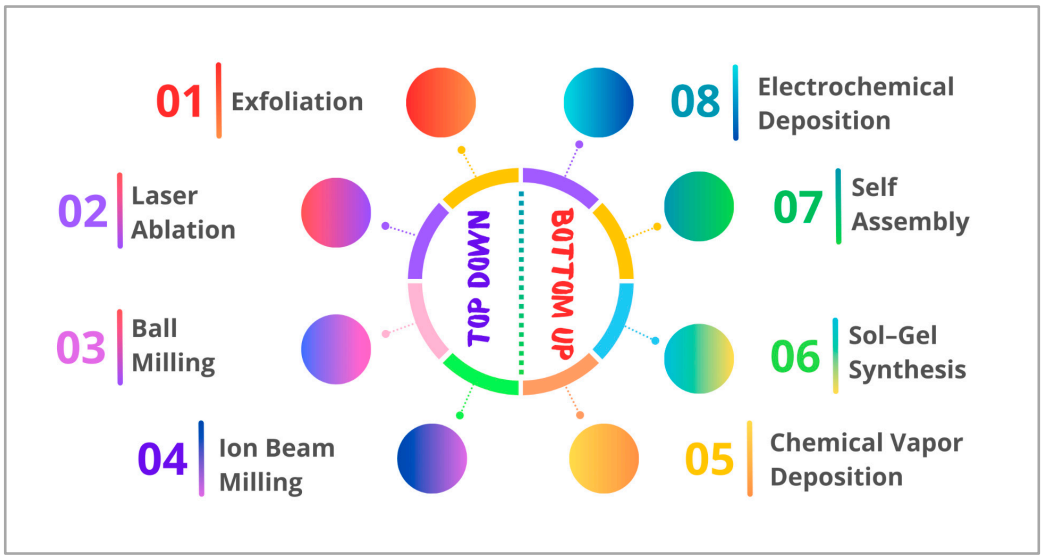

Figure 6. Diagrammatic representation of top-down and bottom-up approaches for synthesis of organic materials.

Table 3. Comparison between bottom-up and top-down deposition techniques.

Technique	Deposition/Synthesis Process	Strength	Weaknesses	Key Features
		Top-Down		
Exfoliation	Mechanically separating layers from bulk material (e.g., tape- or liquid-based exfoliation)	Simple and cost-effective for thin layers	Difficult to control layer thickness, may introduce defects	Produces few-layer 2D materials; Thickness control: ~1–10 nm, layer quality varies
Laser Ablation	High-power laser pulses ablate material from a target to form nanoparticles	High precision, can target specific areas	Expensive, requires specialized equipment	Pulse width: ~ns–fs, laser fluence: ~0.1–10 J/cm^2; Ideal for nanoparticle synthesis
Ball Milling	Mechanical milling of bulk material into smaller particles using rotating balls	Scalable, produces nanoparticles of varying sizes	May lead to contamination, difficult to control particle size distribution	Particle size: 10–100 nm, milling speed: 300–500 rpm; Efficient for nanopowder production
Focused Ion Beam (FIB) Milling	Ion beam bombards material, removing surface atoms for patterning	High resolution, allows for detailed patterning	Time-consuming, expensive, potential sample damage	Beam current: ~10 pA–20 nA, ion beam diameter: ~10 nm; Precise nano-structuring

Table 3. *Cont.*

Technique	Deposition/Synthesis Process	Strength	Weaknesses	Key Features
		Bottom-Up		
Chemical Vapor Deposition (CVD)	Gaseous precursors react/decompose on a heated substrate to form thin films	Produces high-quality films, good control over thickness and composition	Requires high temperatures, expensive precursors	Deposition temp: ~500–1000 °C, pressure: ~1–10 Torr, growth rate: ~1–10 µm/h; Ideal for thin films and nanomaterials
Sol–Gel Process	Chemical solution (sol) transitions into a gel and then dried to form a solid	Low-temperature synthesis, good control over particle size	Long processing times, potential for cracks in final films	Particle size: ~10–50 nm, drying temp: ~100–200 °C, processing time: ~24–48 h; Suitable for nanocoating
Molecular Self-Assembly	Molecules spontaneously organize into structured, ordered patterns	Precise control over structure, forms highly ordered systems	Limited to specific materials and conditions	Assembly time: ~1–12 h, feature size: ~1–10 nm; Applicable for nanoscale molecular systems
Electrochemical Deposition	Ions are reduced at an electrode surface to deposit material (often metal–organic)	Low-cost, easy to scale, good control over thickness	Requires conductive substrates, may need post-treatment	Deposition voltage: ~1–3 V, current density: ~10–50 mA/cm^2, film thickness: ~10–500 nm; Used for coatings and films

Deposition and synthesis methods, such as spin coating, vapor deposition, and inkjet printing, are commonly used across various optoelectronic devices. However, the requirements for each technique often vary depending on the specific application. For instance, while spin coating may be suitable for fabricating thin films in OSCs, OLEDs might require more precise vapor deposition to achieve the desired film uniformity and thickness. Optimization of these synthesis methods for each device ensures that organic materials meet the specific needs of the target application while retaining their versatility.

4.1. Top-Down Methods

4.1.1. Exfoliation

A crucial process called exfoliation occurs when layered materials expand owing to external influences such as chemical or physical forces, as shown in Figure 7a, which reduce the strength of the non-covalent connections between the layers. These materials are split into sheets with one or more layers, offering a unique opportunity to create thin, excellent-quality layers from bulk materials [73]. The two main types of exfoliation methods are physical and chemical methods. Chemical exfoliation facilitates layer separation by changing the chemical structure of the precursor material via appropriate reaction pathways. Owing to its ability to modify the surface chemistry, this method is particularly useful for creating functionalized materials with certain properties. However, on rare occasions, these chemical alterations may affect the intrinsic properties of the material. Conversely, physical exfoliation removes the layers while maintaining the fundamental properties of the material by applying mechanical or external forces. This method is ideal for circumstances requiring material integrity because it maintains the flawless structure and performance of the organic material while generating no visible deterioration.

Both chemical and physical exfoliation processes can be used to produce exfoliated organic materials on a large scale in a straightforward and efficient manner [74]. Particularly, in the fields of energy storage, catalysis, and environmental cleanup, these methods are popular because of their scalability and simplicity of use. Owing to their increased surface area, unique electrical properties, and chemical durability, exfoliated organic molecules have become more valuable in a variety of applications, particularly in the energy and environmental sectors [75].

4.1.2. Laser Ablation

Laser ablation is another method of producing organic nanoparticles from organic microcrystalline powders in a weak solvent, as illustrated in Figure 7b. The advantage of this process is that it does not require any extra materials or chemical reagents; instead, the powdered sample is immediately converted into a stable colloidal solution. It is possible to precisely regulate the size, shape, and phase of the resultant nanoparticles by adjusting the laser wavelength, pulse width, fluence, and total number of laser shots. This procedure involves exposing organic microcrystals floating in water to intense laser pulses, which break them apart. When the released particles are swiftly gathered and stabilized in the surrounding water, stable nanocolloids are formed [76,77]. By altering the laser settings, this method can be utilized to precisely and versatilely adjust the characteristics of nanoparticles.

One of the primary advantages of laser ablation is its considerable control over nanoparticle production. By accurately adjusting the laser pulse width, wavelength, fluence, and shot number, researchers can perfectly regulate the size distribution and phase composition of nanoparticles. This level of control is necessary for producing high-quality organic nanoparticles because application-specific requirements require precise regulation of the particle size, shape, and phase. Laser ablation is a neat and effective top-down technique for creating nanoparticles. The contamination risk is low because no additional chemicals or solvents are used. Due to the inherent non-contact nature of the process, the produced nanoparticles are shielded from external impurities [78]. Furthermore, the stability and purity of the nanoparticles can be further improved by collecting them in a controlled atmosphere without being exposed to air, owing to their ability to perform ablation in a weak solvent. Thus, this technique has created new opportunities for the synthesis of organic nanoparticles, particularly in applications where extreme purity and precision are essential.

4.1.3. Ball Milling

Mechanochemical approaches to organic synthesis have attracted considerable attention because of their many uses in green chemistry. These techniques have multiple benefits because they expand the surface area and areas of contact between reactants by exerting mechanical forces on different reactants. As a result of this increase in effective collisions, reaction paths become more available, and reaction efficiency increases. Ball milling is based on the application of external mechanical force. More specifically, mechanical energy is produced by the alternating impacts of the reactant particles, grinding tank, and grinding balls. As a result, the particles are continually deformed, squeezed, and broken into smaller particles (see Figure 7c). This process creates an increased surface contact between the ingredients, which allows the substance to change more efficiently and become more reactive [79,80]. Ball milling has attracted considerable attention in the field of organic synthesis because of its capacity to enable reactions at room temperature, without the need for solvents, and under moderate circumstances. It can be used in a wide range of organic processes, including those that result in the formation of carbon–carbon and carbon–heteroatom bonds, which are necessary for the synthesis of complex molecules. Moreover, ball milling is necessary for the production of these compounds, which is crucial for both academic studies and the pharmaceutical industry, because heterocyclic compounds are prevalent in physiologically active substances [81].

4.1.4. Focused Ion Beam Milling

Intermediate chemical processes are often required for other nanofabrication methods, such as polymer spin coating or reactive etching. Nevertheless, the material is physically removed using focused ion beam (FIB) milling (see Figure 7d), which employs the direct impact of ions [82]. The capacity of this method to solve problems with chemical compatibility is one of its main features, which makes it adaptable to a variety of materials. Using electron microscopy, operators can observe FIB milling in real time, giving them perfect

control over the milling beam and enabling extremely accurate material sculpting [83]. Li et al. used the organic semiconductor molecule perylene in single crystals to generate two-dimensional patterns using FIB milling. Applying an ultrathin gold (Au) covering helps shield these fragile organic crystals from the harm caused by electron beams during the milling process. Following milling, the protective layer was carefully removed using a potassium iodide/iodine (KI/I2) etchant solution, revealing the crystal structure without jeopardizing its stability. It is essential to take this precautionary measure because it protects the crystal from potential harm from the high-energy electron beam while still enabling the imaging of the crystal in the FIB device. With this technique, features may be created that have a spatial resolution of approximately 130 nm and preserve up to 90% of the initial photoluminescence intensity in the surrounding crystal areas, which can be obtained. This retention of photoluminescence is vital, especially in optoelectronic devices, where the optical characteristics of the material must be maintained. These proof-of-concept studies show that FIB milling has the potential to be an effective technique for regulating the nanoscale shape of organic molecule crystals, opening new possibilities for the creation of highly accurate nanoscale electronics [84].

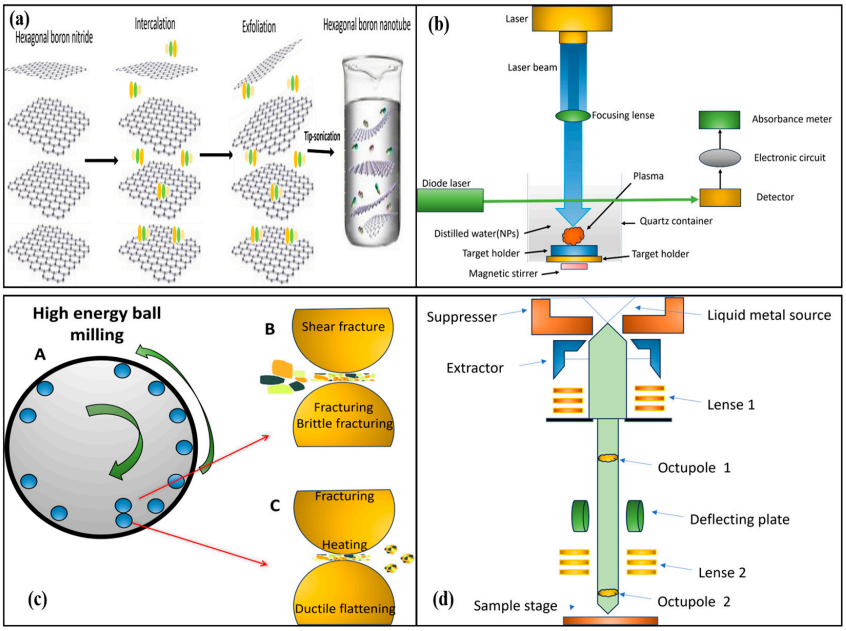

Figure 7. Diagrammatic representation of top-down approaches for the synthesis of organic compounds. (**a**) Exfoliation [73], (**b**) laser ablation [76], (**c**) ball milling [80], and (**d**) ion beam milling [84].

4.2. Bottom-Up Approaches

4.2.1. Chemical Vapor Deposition

Chemical vapor deposition (CVD) is a popular and significant method for creating thin films or nanostructures on an exposed substrate. It works using volatile precursors, as represented in Figure 8a. It is particularly adaptable because it can produce a wide range of organic nanostructures, including nanoparticles, nanotubes, nanofibers, and nanocomposites. The ability of the CVD process to produce thin films of consistent quality and fine control over their composition and morphology has led to its adoption as a unique manufacturing technique in a number of industrial areas.

Numerous studies have shown that organic compounds produced by chemical vapor deposition (CVD) have advantages over those produced by wet chemical techniques. The CVD technique yields organic compounds with significant advantages when used, as evidenced by combustion catalysis [85] and selective reactions [86]. The main reason for this is that the CVD method can yield an active material that is more broadly dispersed and has stronger interactions with the support matrix, leading to increased performance.

Owing to their excellent adhesion to substrates and high degree of uniformity, CVD-generated organic compounds are especially valuable for a range of electrical and catalytic applications. As per scientific definitions, chemical vapor deposition (CVD) is a process that creates a thin solid layer on a substrate by reacting gaseous precursors. CVD is a reactive process, as opposed to Physical Vapor Deposition (PVD) methods, including evaporation, sputtering, or sublimation. This difference stems from the fact that in CVD, the desired material grows on the substrate as a result of chemical processes that occur in the gas phase and produce the deposited material. Gaseous species either disintegrate or react at high temperatures, leaving behind a solid thin film as a byproduct of the reaction.

CVD has many benefits when used with organic materials, particularly in the creation of sophisticated organic nanostructures for optoelectronics, electronics, and sensors. Because CVD allows for the exact tuning of growth conditions, the organic nanomaterials produced have higher electrical characteristics and better integration with different substrates [87].

4.2.2. Sol–Gel Synthesis

The sol–gel process is a widely used chemical method, particularly a wet chemical approach, for the synthesis of various nanostructures, including organic nanoparticles (see Figure 8b). To create a gel, this process involves dissolving a molecular precursor in a solvent such as water or alcohol, and heating and stirring the mixture to cause hydrolysis or alcoholysis. Depending on the desired qualities and the planned use of the finished product, the reaction produces a gel that is initially wet or moist and must be dried using proper processes. For example, in an alcoholic solution, drying can be achieved by burning the alcohol. After drying, the resulting gels are often ground into powder and heated to very high temperatures to remove any remaining organic matter and enhance the structural properties of the material. The sol–gel method is widely known to be cost-effective and offers superior control over the chemical composition of the final products owing to its relatively low reaction temperatures [88]. Materials fabricated by the sol–gel process are widely used in many different sectors [89,90]. These industries include energy storage, surface engineering, biosensors, optical and electrical technologies, medicinal applications, and separation technologies, such as chromatography. The sol–gel approach is a unique commercial process for producing nanoparticles with various chemical compositions. It is an essential technique in contemporary materials research because of its versatility and fine control over the particle size, morphology, and chemical purity.

4.2.3. Molecular Self-Assembly

Molecular self-assembly is the process by which molecules interact with one another to construct molecular building blocks into nanostructures and materials, as illustrated in Figure 8c. By using this method in conjunction with careful control over the solution assembly routes, desirable structures with specific characteristics can be built. The versatility and potential of molecular self-assembly to produce materials with functionalities has drawn a lot of interest from a wide range of fields. One major factor contributing to its enormous potential is its capacity to store a wide range of compounds.

When organic molecules are used as building blocks for molecular self-assembly, the adaptability of organic synthesis gives them an edge [91]. In addition to their specific roles in molecular devices, these building blocks can be functionalized with groups that aid in regulating the self-assembly process. The system can test different binding geometries until it reaches a thermodynamically stable equilibrium because the process depends on reversible bond formation [92]. To do this, important interactions such as hydrogen bonds, weak electrostatic interactions, and van der Waals forces are essential. Hydrogen bonds provide more selective control than van der Waals and electrostatic forces, allowing for the production of a wide range of shapes, even at the single-molecule level [93].

Molecular–surface interactions further affect molecular self-assembly at surfaces, providing an additional level of control over the development of structures. Structural

variety at surfaces is contingent upon striking a balance between surface and intermolecular contacts, as this interaction expands the scope of potential structures beyond that observed in bulk molecular groupings.

4.2.4. Electrochemical Deposition

Among the most promising approaches for creating organic materials, electrochemical methods are widely acknowledged [94]. These techniques not only produce organic molecules in powder form on a massive scale, but also work quite well for fabricating coatings and thin films (see Figure 8d). The numerous benefits of electrochemical deposition make it an appealing choice for industrial and research applications. One of the main advantages of this method is that it does not require any pre-treatment; all that is needed before the process starts is quick cleaning of the substrate. It also requires less energy and is efficient because it runs under mild conditions and has quick synthesis periods. The ability to monitor and regulate the process in real time is one of the most significant characteristics of electrochemical synthesis. This feature is particularly beneficial in large-scale industrial production. Further, ensuring homogenous films with great throwing force and fewer cracks is the self-closing characteristic of the deposition process, which raises the caliber of the final product [95].

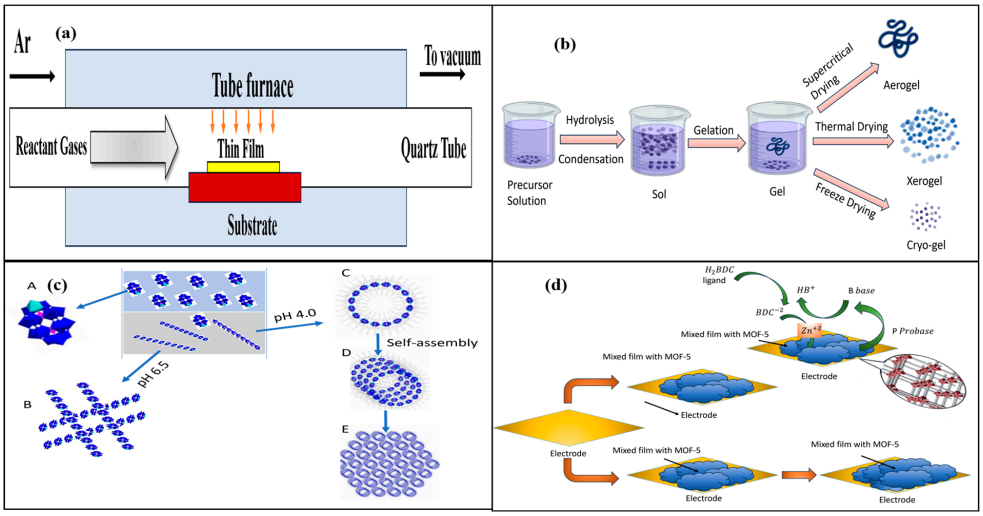

Figure 8. Diagrammatic representation of bottom-up approaches for the synthesis of organic compounds, (**a**) CVD [87], (**b**) sol–gel [88], (**c**) molecular self-assembly [91], and (**d**) electrochemical deposition [95].

The first step in the electrochemical synthesis process was the preparation of an electrolyte solution containing the required organic material precursors. The electrodes were arranged in an electrochemical cell and were connected to an electrochemical workstation. The electrodes consisted of a working electrode, a counter electrode, and a reference electrode. An electric potential or current was delivered across the cell during deposition, which reduced the number of ions and formed a film or nanoparticle on the working electrode. The exact control that electrochemical techniques provide over the particle size and shape is one of their main advantages. Researchers may fine-tune the process to produce materials with unique properties adapted to various applications, from electronics to coatings, by varying important factors including current density, applied potential, and electrolysis time [96]. The synthesis of high-performance organic materials requires electrochemical technologies, which are indispensable because of their precision and adaptability.

5. Application of Organic Materials

Organic materials find applications in a variety of optoelectronic devices, including OSCs, OLEDs, organic field-effect transistors (OFETs), and organic photodetectors (OPDs). Despite the diversity of these devices, the same materials often face similar challenges,

such as stability under ambient conditions and the need for efficient charge transport. For example, in OSCs, organic materials must ensure high efficiency in light absorption and charge separation, while in OLEDs, the focus is on maximizing light emission and color purity. By examining the use of these materials across devices, we can uncover common strategies for overcoming these challenges, such as improving material stability or enhancing charge mobility through doping or molecular design.

5.1. OLEDs

Organic light-emitting diodes (OLEDs) provide substantial advantages over standard LEDs based on inorganic semiconductors. Organic light-emitting diodes (OLEDs) are a revolutionary technology that creates light through organic chemicals, developed from Tang and Van Slyke's groundbreaking research in 1987 [97]. OLEDs have attracted considerable attention because of their remarkable use as eco-friendly light sources and full-color display screens. Under an external voltage, OLEDs, which are electroluminescent devices, can emit light within an organic emissive layer. Their benefits include the potential to reduce manufacturing costs, light weight, versatility for a range of applications, and ability to be produced on a variety of substrates using solution-based techniques. Furthermore, OLEDs are very appealing to academia and industry because of their low driving voltage, quick reaction, and simple preparation [98]. OLEDs are ideal for both consumer electronics and lighting applications because they harness the light emission characteristics of organic materials to create high-quality displays with exceptional color purity and energy economy [99,100].

5.1.1. Basic Principles and Structure

OLEDs usually have a multilayered construction that is intended to maintain the electron and hole recombination sites contained in the emissive layer of the device. In general, the device consists of the following components: a transparent conductive glass substrate with a high work function, transparent anode, electron and hole transport layer (ETL and HTL), electron and hole injection layer (EIL and HIL), emission layer (EML), and cathode (Figure 9a) [101]. The stacking of the organic layers improves device performance, the injection layers help to prolong the lifespan of the device, and the transport layers reduce power consumption and increase efficiency [102]. OLEDs produce mobile electrons and holes when a voltage is applied, causing an electrical current to flow across them. The emissive layer receives electrons from the cathode and the EML (Figure 9b) becomes exciton-paired because of the holes injected from the anode [102].

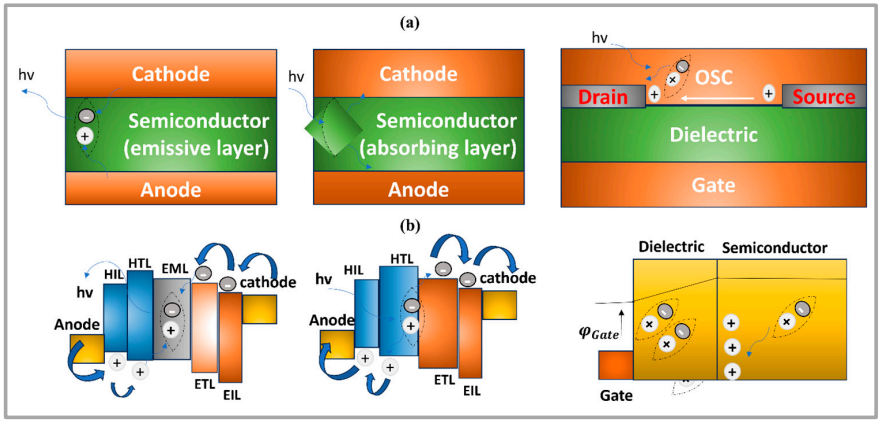

Figure 9. (**a**) Schematics, (**b**) energy band diagrams, and working mechanism of OLEDs [101].

5.1.2. Working Mechanism

OLEDs work by using a process called electroluminescence, in which light is produced when electrons and holes in the emissive layer recombine (Figure 9). The electric field generated by the application of voltage across the OLED structure causes the holes to be

injected into the organic layers from the anode and the electrons injected from the cathode to migrate toward one another. Light is produced when an electron recombines with a hole in the emissive layer, thereby releasing energy during the process. The energy bandgap of the organic material utilized in the emissive layer determines the hue of light. The following formula can be used to approximate the OLED device brightness (L) [103,104]:

$$L = \eta \cdot q \cdot \mu \cdot V \cdot F \quad (1)$$

where q is the elementary charge, μ is the mobility of the charge carriers, V is the applied voltage, F is the factor accounting for the ratio of holes to electrons, and η is the quantum efficiency (the proportion of electrons that recombine to generate light).

Figure 10a shows the J-V data for various OLED samples. It is noteworthy that all devices demonstrated an outstanding low turn-on voltage (Von) between 4 and 5 V, given their two-organic layer construction. Devices with an external quantum efficiency (EQE) of 10.5%, a maximum current efficiency (ηcmax) of 20.0 cd A^{-1}, a maximum power efficiency (ηpmax) of 8.7 Â lm W^{-1}, and a maximum brightness of 4030 cd m^{-2} showed solid performance when THF was employed as the solvent for the active layer. With toluene as the solvent, the top-performing devices achieved a maximum brightness of 3240 cd m^{-2}, ηcmax of 24.3 cd A^{-1}, $\eta_P$max of 16.9 lm W^{-1}, and a maximum EQE of 14%, which is comparable to the best values reported in the literature for devices with more complex structures. For this straightforward structure, the toluene-based device likewise showed the lowest Von and best balance between power and current efficiency, resulting in an ideal EQE.

Figure 10b presents the comparative EQE data as functions of brightness. A low roll-off was observed, particularly in the device using chloroform as the solvent, with only 1% roll-off at maximum brightness and 1000 cd m^{-2}. In contrast, the device using toluene showed the highest roll-off at 32%, while the THF-based device had a roll-off of 25%, and the chlorobenzene-based device exhibited a roll-off of 6%. These results indicate that the devices remained stable up to 1000 cd m^{-2} without the use of blocking layers, maintaining high brightness and stability under increased voltages [104].

The remarkable performance of the OLED with a 40 nm layer of the derivative is demonstrated by the luminance–voltage and current efficiency–luminance characteristics of the devices ITO/PEDOT/HTL of 3,3-di[3-(4-fluorophenyl) carbazol-9-yl]methyloxetane (40–60–80 nm)/Alq_3/LiF/Al, as shown in Figure 10c,d. This device had a maximum brightness of more than 21,000 cd/m^2, a high luminous efficiency of 4.7 cd/A, a power efficiency of 2.6 lm/W, and a turn-on voltage of 3.9 V. These findings verify that the performance of the device was greatly improved by the addition of an HI-TL in conjunction with the HTL of 3,3-di[3-(4-fluorophenyl) carbazol-9-yl]methyloxetane. All things considered, the OLEDs described here show exceptionally high efficiencies [105].

Figure 10d displays the electroluminescent spectra of the OLEDs, with the conjugated polymers acting as hole transporting layers (HTLs) at several voltages (7–10 V). According to the findings, the polymers successfully performed their roles as hole-carrying layers without creating an exciplex at the Alq_3 emitter interface. Furthermore, effective charge-carrier recombination of the Alq_3 emitter layer was enabled by both hole injection and mobility in the thin films of these polymers. Another characteristic OLED behavior is illustrated by the current density–voltage (I–V) curves in Figure 10e, which have low turn-on voltages of 3.0 V for the device utilizing polymer 9 as HTL; as this polymer has better performance and a lower turn-on voltage, it is a good choice for OLED applications because of its improved hole transport qualities [106].

De Silva et al. investigated the synthesis and characterization of three multifunctional compounds (A, B, and C) designed to improve the performance of organic light-emitting diodes (OLEDs). These compounds incorporated pyrene and benzimidazole moieties, which were strategically selected to reduce π-π stacking through steric hindrance, thereby decreasing the crystallinity and limiting intermolecular aggregation. The study found that compound B exhibited the most favorable photophysical properties, achieving an

external quantum efficiency (EQE) of 4.3% at 3.5 V and a luminance of 290 cd/m^2 at 7.5 V, as illustrated in Figure 10f. By improving charge transfer and stability, the results showed that these pyrene-benzimidazole derivatives might function as blue emitters and mitigate the inefficiencies often observed in conventional blue OLEDs. The materials for OLED technology have advanced as a result of this study, which is important for enhancing display quality and prolonging the lifespan of consumer gadgets [107].

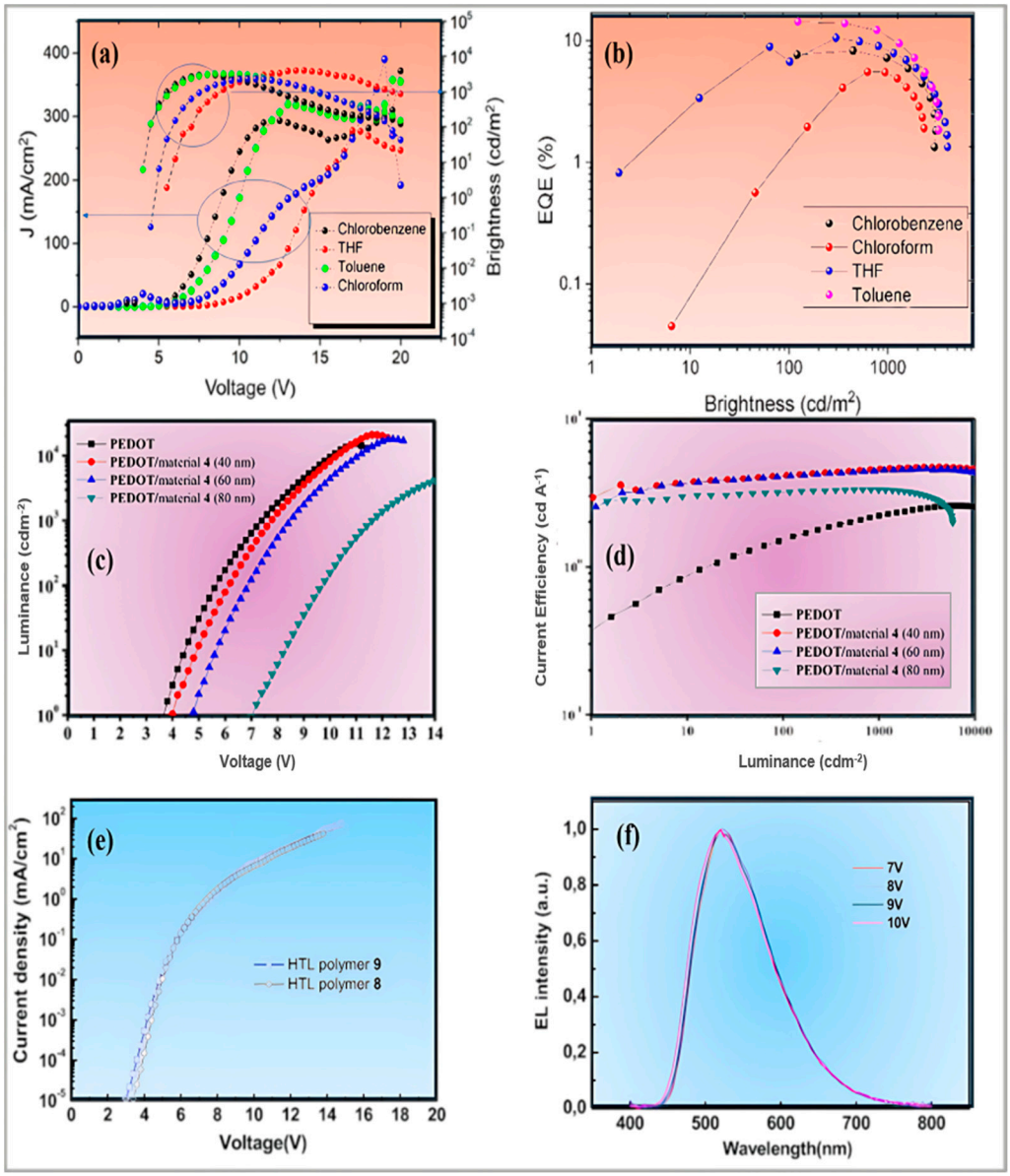

Figure 10. (**a**) J−V data for the different OLED samples, (**b**) EQE data as functions of brightness, (**c**) the luminance–voltage and (**d**) current efficiency–luminance characteristics of the devices, (**e**) current density–voltage (I−V) curves of OLEDs, and (**f**) the electroluminescent spectra of OLEDs [104–106].

For 2-phenylpyrimidine derivatives containing triphenylamino or 4,4′-dimethoxytriphenylamino donor moieties, thermal, electrochemical, photophysical, charge-transport, and electroluminescent properties were studied. In the solid films, the emission shifted from blue (460 nm) to green-blue (513 nm) upon the addition of diphenylamino moieties using methoxy groups. Furthermore, the hole drift mobility increased significantly to 4.9 × 10^{-5} cm^2/V·s in an electric field of 9.2 × 10^5 V/cm. The improved charge balance in the 4,6-bis(4-di(4-methoxyphenyl) amino) phenyl)-2-phenylpyrimidine layers is responsible for the higher overall efficiency of devices with both neat and guest host systems using the methoxy-containing emitter, even though

the compound without methoxy groups demonstrated more efficient emission and better OLED performance [108].

5.2. Organic Photodetectors

Organic photodetectors (OPDs), which use organic materials to convert light into electrical signals, have become an essential optoelectronic technology. These devices are made possible by the special properties of organic semiconductors, which include their flexibility, lightweight design, and potential for affordable large-scale production. OPDs offer significant benefits in situations where typical inorganic photodetectors are limited, making them ideal for a wide range of applications, from imaging to environmental monitoring. This figure shows the device setup and energy-band diagram of an OPD [109].

5.2.1. Basic Principles and Structure

The fundamental process by which organic photodetectors work is to absorb photons and converting them into electrical charges or current. The three main components of an OPD are the substrate, active organic layer, and electrodes. Depending on its intended use, a substrate may be made of flexible polymers or glass. Light absorption and charge production in the active organic layer were carried out using small molecules or semiconducting polymers. These materials were selected because of their ability to effectively absorb light and form excitons, which are the bonded pairs of electrons and holes. Indium tin oxide (ITO) was frequently used as an transparent electrode in OPDs on top of the basic material. Next, the charge transport layer was placed between the active organic layer and the top electrode made of aluminum or silver. The interface between the electrodes and organic layer affected the overall performance of the device. The efficient extraction of the generated charges depends on this interface.

5.2.2. Working Mechanism

The functioning of an organic photodetector involves several crucial processes such as light absorption, charge separation, charge transfer, exciton production, and exciton diffusion as shown in Figure 11. When light enters an organic material and stimulates electrons to move from their ground state to a higher energy state, excitons are produced. These excitons must go to the interface between the electron donor and electron acceptor materials in the active layer because they are bound. At this contact, the excitons break into free charge carriers, mostly holes and electrons [110].

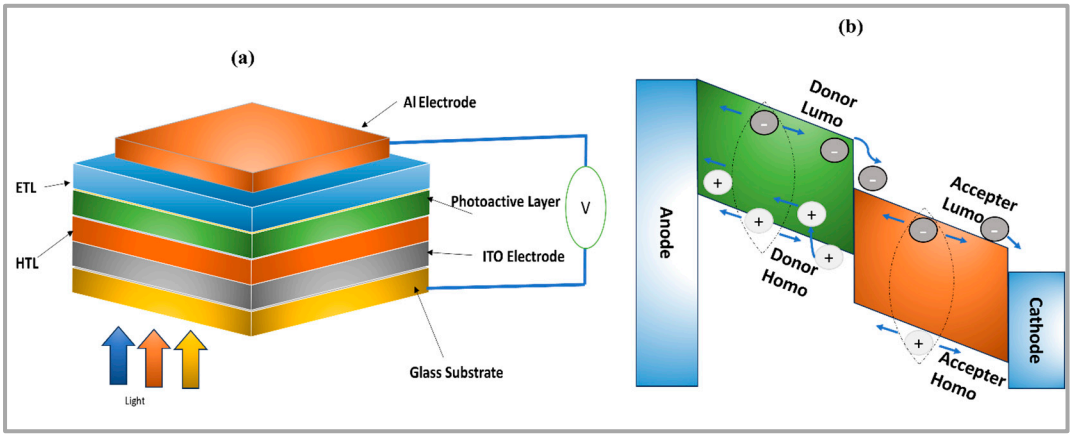

Figure 11. (**a**) Schematics, (**b**) energy band diagrams, and working mechanism of OLEDs [109].

The dissociation process is the energy offset between the donor and acceptor materials, which results in an intrinsic electric field. This field separates the electron–hole pairs and moves them to the appropriate electrodes. The accumulation of free carriers subsequently generated a photocurrent at the electrodes. The effectiveness of the process depends on a

number of factors, including the mobility of charge carriers, the length of exciton diffusion, and the absorption spectrum of the organic materials.

5.2.3. Understanding Responsivity and Detectivity in Organic Photodetectors

Several techniques can be used to gauge the performance of an organic photodetector. A crucial parameter is the responsivity (R), which measures how efficiently the photodetector transforms light into an electrical signal. Responsivity is defined as the ratio of the photocurrent (J_{ph}) to incident optical power (P_{in}), and it is represented by the equation below [111].

$$R = J_{ph}/P_{in} \quad (2)$$

where P_{in} is the power of the incident light and J_{ph} is the photocurrent produced by the apparatus. A photodetector with higher responsivity can produce a greater photocurrent for a given quantity of incident light because it is a more sensitive device.

The detectivity (D*) of the photodetector, or its capacity to recognize weak light signals, is another crucial metric. Detectivity was defined as [112,113].

$$D^* = R/(2 \cdot q \cdot J_d)^{1/2} \quad (3)$$

The current flowing through the device per unit area in the absence of light is known as the dark current density, and q and J_d represent the elementary charge and current, respectively. Low noise and high sensitivity photodetectors are indicated by high detectivity, which is advantageous for applications requiring the detection of very low-light levels.

Yu et al. employed a ternary mix method to create PM6: BTP-eC9: PCBM–based OPDs with a high response frequency, ultrahigh responsivity, and broad bandwidth (350–950 nm). Utilizing external quantum efficiencies (EQEs) and responsivities (Rs), we can assess the impact of various blend ratios and morphologies. Figure 12f shows that with zero bias, the EQE of the PM6: BTP-C9 binary OPD was approximately 70%. PCBM over-aggregation resulted in an increase in the carrier trap content, which hindered the extraction of free carriers. This is supported by the weaker EQE responses of the 1-PCBM device compared with those of the 0.1-PCBM and 0.5-PCBM OPDs. In order to produce PM6:BTP-eC9, Yeng Yu et al. used a ternary mix technique. At a reverse bias of −1.5 V, the EQE curves of the 0.1-PCBM and 0.5-PCBM OPDs demonstrated EQE increases greater than 10%.

The attributes of OPDs include a broad bandwidth (350–950 nm), high response frequency, and ultrahigh responsiveness. The external quantum efficiencies (EQEs) and responsivities (Rs) of the OPDs were used to determine the effects of the mixing ratios and morphologies. The EQE of the PM6 binary OPD was approximately 70% under zero bias. The 1-PCBM device had a lower EQE, indicating that the greater carrier trap content caused by PCBM over-aggregation impeded the extraction of free carriers. The EQE responses of the 0.5- and 0.1-PCBM OPDs are comparable. EQE increases of over 10% were detected at a reverse bias of −1.5 V in the EQE curves of the 0.1-PCBM and 0.5-PCBM OPDs, with a maximum response of 100% recorded at 860 nm. However, the series carrier injection phenomenon prevented the control and 1-PCBM OPDs from producing adequate EQE responses. The graphs of responsivity (R) at biases of 0 and −1.5 V are shown in Figure 12e. The control, 0.1-PCBM, 0.5-PCBM, and 1-PCBM OPDs had R values of 0.43, 0.45, 0.42, and 0.41 A/W at λmax (860 nm: Rλmax) at 0 V, respectively. For both the 0.1-PCBM and 0.5-PCBM OPDs, the Rλmax values rose to 0.572 and 0.59 A/W under −1.5 V bias, respectively [114].

Zhai et al. proposed a broadband photodetector based on photogenerated holes and charge transfer (PHCT) that utilizes the small-molecule organic semiconductor 8-hydroxyquinolinato aluminum (Alq_3). Known for its use as both an organic light-emitting material and an electron injection material, Alq_3 typically absorbs light at wavelengths shorter than 460 nm. To extend the spectral range of the Alq_3-based photodetector, plasmonic nanostructures were incorporated, providing a cost-effective strategy for the development of infrared photodetectors. Noble metal nanoparticles such as gold (Au) and silver

(Ag) are commonly used to enhance optical absorption and light scattering. Compared with gold, silver has lower resistivity and is less expensive. The broadband PHCT-based photodetector features a configuration of ITO/Alq_3/AgNP/Al, where a thermally evaporated layer of silver nanoparticles (NPs) is positioned between the Alq_3 active layer and aluminum cathode to excite plasmonic resonances.

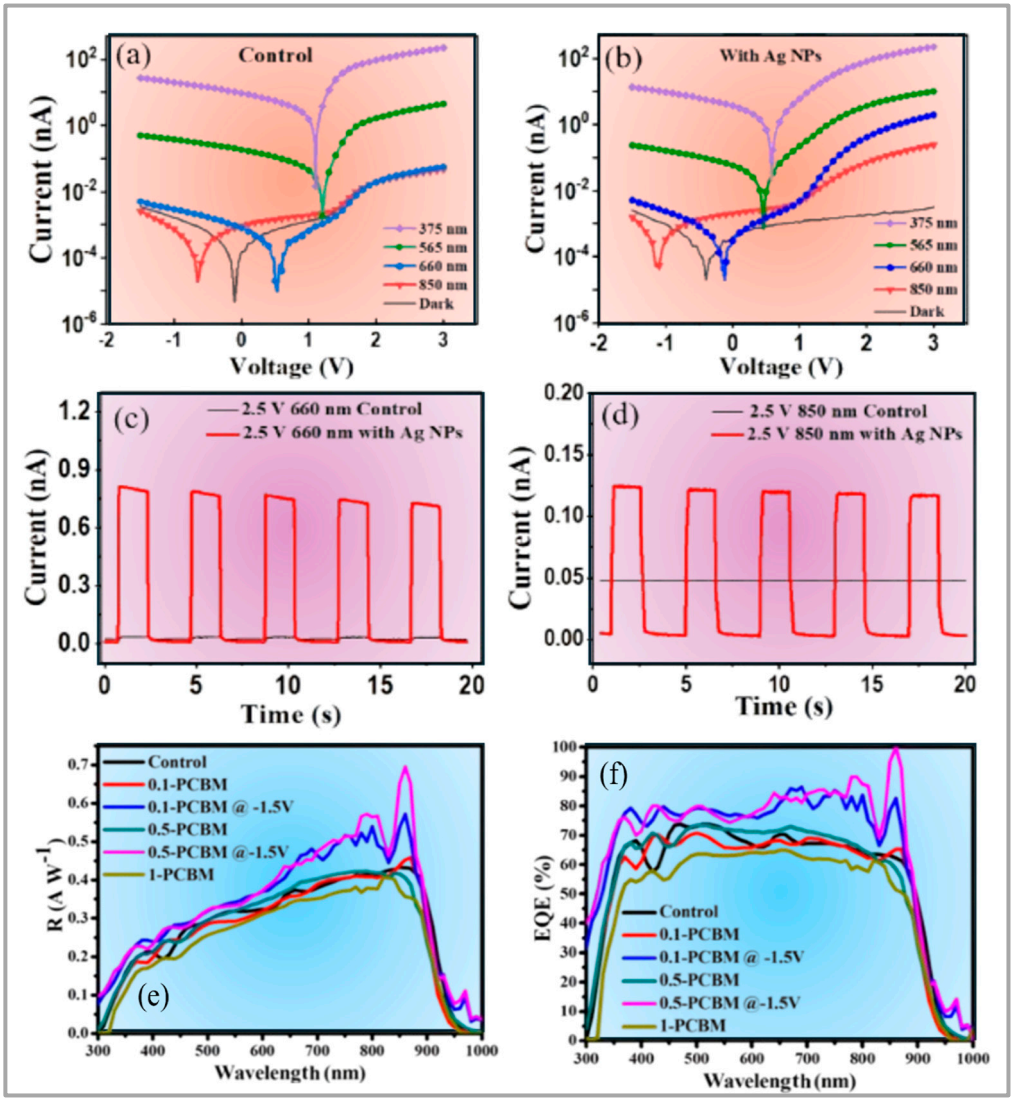

Figure 12. Logarithmic I−V characteristics of control and plasmonic organic photodetectors (OPDs) in dark and under illumination at 375 nm, 565 nm, 660 nm, and 850 nm (**a**,**b**). Transient current responses of various OPDs with 660 nm and 850 nm pulse LEDs (**c**,**d**). Responsivity (R) measured at 0 and −1.5 V (**e**), along with external quantum efficiency (EQE) responses at 0 V for different devices (**f**) [114,115].

Figure 12a,b show the log I–V characteristics of both the control and plasmonic photodetectors under illumination at different wavelengths: 375 nm (rectangles), 565 nm (circles), 660 nm (diamonds), and 850 nm (triangles), with an incident power density of 13 mW/cm^2. For the control photodetector, the photocurrents at wavelengths of 660 and 850 nm, with biases above 1.8 V, were nearly indistinguishable from the dark current, as shown in Figure 12a. This result aligns with the transient photocurrent responses shown by the thin curves in Figure 12c,d, indicating that the control photodetector at 2.5 V does not produce any electric signals under 660 nm or 850 nm pulse illumination. In contrast, the plasmonic photodetector exhibited photocurrents distinct from its dark currents at 660 nm and 850 nm, even at biases above 1.8 V, as shown in Figure 12b. The transient photocurrent

responses of the plasmonic photodetector under pulse illumination, depicted by the thick curves in Figure 12c,d, confirm that the incorporation of AgNPs allowed the device to effectively detect light at longer wavelengths which are beyond the intrinsic absorption band of Alq_3. At 2.5 V, the photo-to-dark current ratio at 660 nm was 479, corresponding to a responsivity of 2.01×10^{-6} A/W, while at 850 nm, the ratio was 67, corresponding to a responsivity of 0.28×10^{-6} A/W [115].

Using a perovskite/organic heterojunction design, Saleem et al. demonstrated a novel method for creating photodetectors that function in the near-infrared (NIR) region. The responsivity and spectral response properties of these photodetectors were analyzed using Technology Computer-Aided Design (TCAD) simulations. A peak responsivity of 0.3 A/W with a full width at half maximum (FWHM) of 37 nm was obtained by adjusting the thickness and trap density of the organic layer according to the significant results. These findings highlight the need to reduce trap densities to improve performance, as the research showed a 170% increase in responsivity with a 10% reduction in trap density. The results suggest that advancements in processing methods might yield organic semiconductors with reduced trap densities and enhanced crystallinity, increasing the potency of NIR photodetectors [116].

Khariani employed vanadyl 2,11,20,29-tetra tert-butyl 2,3-naphthalocyanine (VTTBNc) as the p-type material. The results were reported experimentally on a bulk heterojunction organic photodiode processed in solution after it was mixed with two different acceptors, PC BM and PC BM. The performance of the OPD was evaluated using a range of tests and measurements. A solar simulator was used to obtain the current–voltage characteristics and calculate the external quantum efficiency (EQE). The absorption spectra of the photoactive layers were examined using UV–visible (UV–Vis) spectroscopy. Measurements for different VTTBNc:PC BM ratios showed that the VTTBNc:1.0 blend had lower or quicker responses and recovery durations than the VTTBNc:PC BM (1:1.5) mix. Both photoluminescence and Raman spectra were used to examine the behavior of the ideal mix ratios. The results provide information on the performance of the organic photodiode and the various mix ratios that affect the response and recovery times [117].

5.3. Organic Photovoltaic Cells (OPVs)

Organic photovoltaic cells (OPVs) are a potential method for producing power from sunlight. OPVs use organic molecules or polymers, as opposed to conventional silicon-based solar cells, to transform photons into electrical currents [118]. This organic approach offers several benefits, including the ability to be produced using solution-based techniques on flexible substrates, versatility for a variety of applications, and cheaper production costs.

5.3.1. Basic Principles and Structure

The fundamental components of an OPV are typically transparent conductive substrates (such as indium tin oxide (ITO)), a photoactive layer composed of a combination of electron-donating (D) and electron-accepting (A) materials, and metal electrodes (such as silver or aluminum) for charge extraction, as shown in Figure 13a. Since the active layer absorbs photons and, when exposed to sunlight, produces excitons (bound electron–hole pairs), it is essential. Carefully selected donor and acceptor materials enable effective exciton dissociation and charge transfer [119].

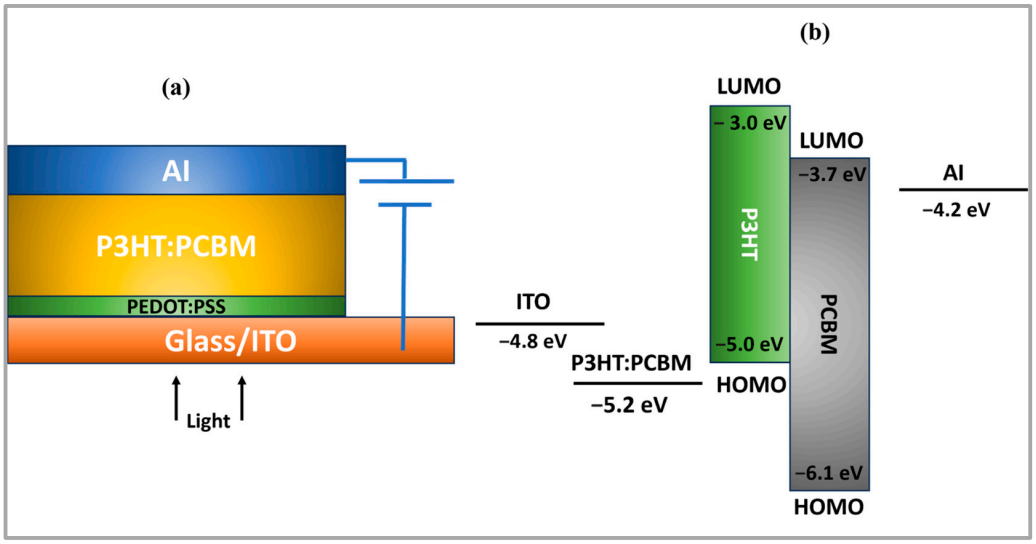

Figure 13. (**a**) Schematics, (**b**) energy band diagrams, and working mechanism of organic solar cell [118].

5.3.2. Working Mechanism

The process by which OPVs operate starts with photons being absorbed by the photoactive layer, as shown in Figure 13b, producing excitons. When these excitons reach the D A contact, they diffuse through the photoactive layer and split into free electrons and holes. Subsequently, the electrons and holes are moved along their designated routes, with the electrons moving toward the cathode via the electron transport layer (ETL) and the holes moving toward the anode via the hole transport layer (HTL). An electric current is produced by the movement of these charges [120]. The photocurrent density (J_{ph}) generated by the OPV device can be described by the following equation [121,122]:

$$J_{ph} = q \cdot G \cdot \eta \quad (4)$$

where η is the device's external quantum efficiency (EQE), which is the percentage of absorbed photons that contribute to the photocurrent, G is the incident photon flux, and q is the elementary charge.

A three-layer tandem organic solar cell (OSC), designed to operate at 300 K, incorporates layers with different bandgap energies to optimize the output photocurrent. The Glass/FTO/TiO_2/first absorber/MoO_3/TiO_2/second absorber/WO_3/MoO_3/TiO_2/third absorber/WO_3/Ag structure is a schematic of the structure under investigation. The bandgaps of the top absorber (Eg1), middle absorber (Eg2) and bottom absorber (Eg3) were wide, medium, and low, respectively, with the relationship Eg1 > Eg2 > Eg3.

Figure 14a,b illustrate the effects of temperature on the device parameters. It is evident that the open-circuit voltage (Voc) significantly decreases from 1.00 V to 0.45 V. This drop in Voc was attributed to an increase in the reverse saturation current with temperature. Even if Jsc increased slightly, there was no overall improvement. The small increase in Jsc resulted from the reduction in the bandgap energy (Eg) with increasing temperature, which allowed more photons to be absorbed. However, both the fill factor (FF) and the efficiency (η) decreased with increasing temperature. Specifically, η decreased from 14.33% to 11.40% as the temperature increased from 300 to 400 K, as shown in Figure 14b [123].

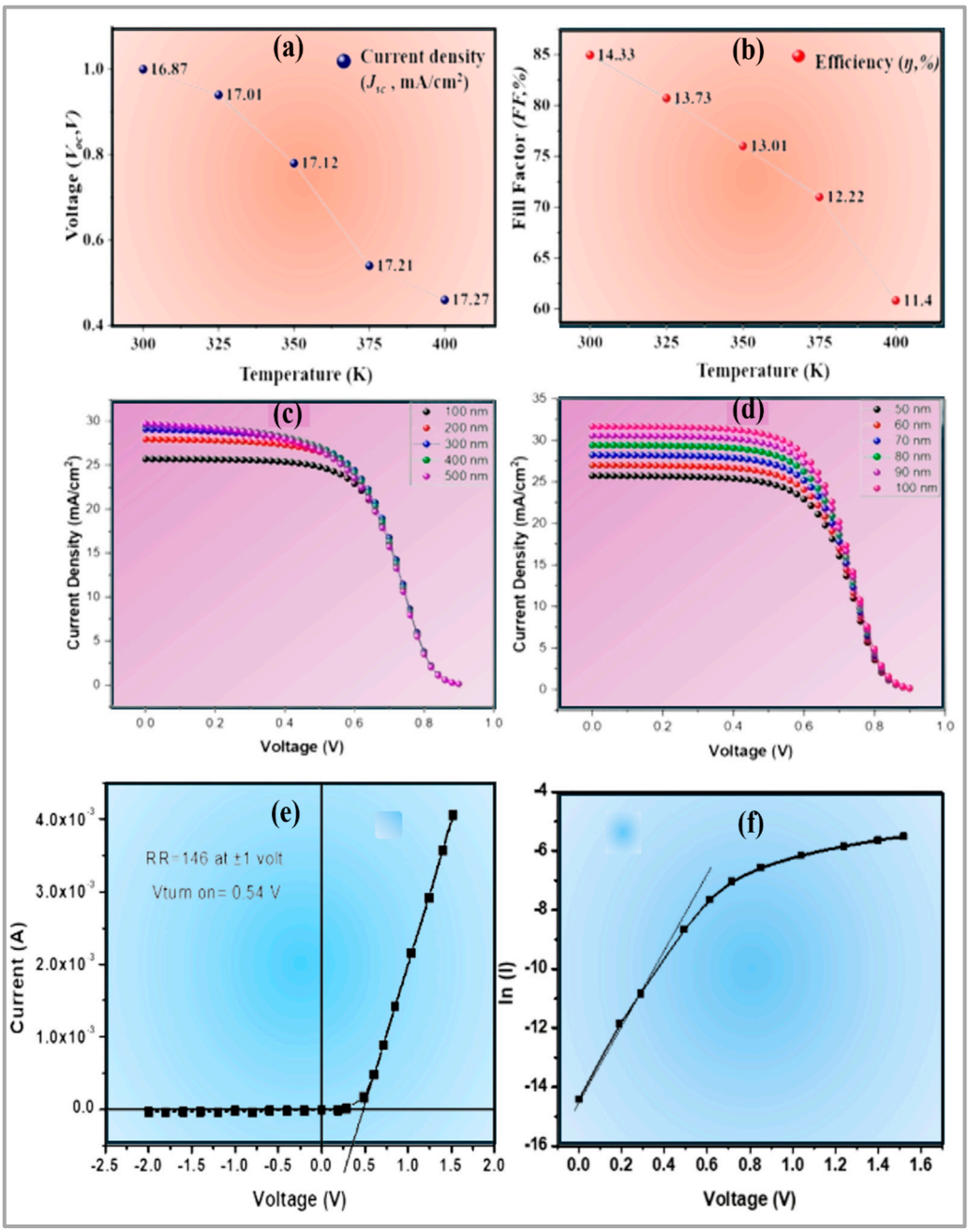

Figure 14. Effect of temperature on key photovoltaic parameters: (**a**) Voc and Jsc; (**b**) FF and efficiency (η). Current density analysis for varying (**c**) absorber layer thickness and (**d**) HTM layer thickness. I−V characteristics of the Ag/ZnPc/PEDOT/ITO solar cell displayed (**e**) under dark conditions and (**f**) in semi-logarithmic form [123–125].

Nowsherwan et al. investigated the replacement of the conventional hole transport layer (HTL) material PEDOT:PSS with graphene oxide to address the stability issues associated with the acidic nature of PEDOT:PSS. Graphene oxide, which is known for its stability and improved performance, was compared with that of PEDOT:PSS. The study also explored the effects of pairing graphene oxide with various active layer materials and examined the impact on essential organic solar cell (OSC) parameters to enhance performance. The functionality and output of a device depend on the thickness of the active layer. Nowsherwan et al. maintained all other parameters at a constant while varying the active layer thickness between 100 and 300 nm and examined the effects on device performance. Figure 14c,d show that as the active layer thickness increased from

100 nm to 200 nm, the output parameters Jsc, Voc, and PCE significantly improved. A larger concentration of electron–hole pairs produced by increased photon absorption in the thicker layer was responsible for this enhancement. However, as the layer thickness increased from 300 to 500 nm, Voc and PCE gradually declined owing to an extended charge carrier diffusion length and a higher recombination rate. For the 300 nm thick device, the maximum Jsc observed was 29.75 mA/cm^2. The FF decreased from 58.45% to 52.06% as the layer thickness increased from 100 nm to 300 nm. This decrease was probably the result of the greater series resistance of the thicker active layer, which limited the capacity of the cell to transfer all of its available power to the electrical load [124].

A ZnPc-based solar cell with Ag and PEDOT/ITO electrodes sandwiching the ZnPc active layer, forming an Ag/ZnPc/PEDOT/ITO structure with PEDOT acting as the hole transport layer (HTL), was studied by Zahoor et al. for its photovoltaic characteristics. The I-V characteristics of the Ag/ZnPc/PEDOT/ITO solar cell tested at room temperature in the dark are shown in Figure 14e. The key device properties, including the rectification ratio (RR), ideality factor (n), reverse saturation current (Io), series resistance (Rs), shunt resistance (Rsh), and barrier height (ϕb), were determined from the I-V curves. The creation of a non-ohmic junction was confirmed by the asymmetrical I-V characteristics, which exhibited a rectifying behavior. From the I-V graph, the rectification ratio was 146 at ±1 V, and the turn-on voltage (Vturn on) was measured at 0.54 V. The characteristics of the organic active layer were responsible for the exponential behavior of the I-V curves in the forward region.

The semi-logarithmic I-V characteristics, which were utilized to calculate the reverse saturation current, barrier height, and ideality factor, are displayed in Figure 14f. These metrics were used to evaluate the quality of the ITO-ZnPc heterojunction interface. When a metal comes in contact with a semiconductor, thermionic emission is usually followed by a forward current. The ideality factor (n), reverse saturation current (I_o), and barrier height (ϕ_b) were determined to be 0.92 eV, 3.8, and 5.5 × 10^{-7} A, respectively, based on the ln(I)–V characteristics. The ideality factor in this instance deviated significantly from unity, which was in contrast to the ideal value, indicating that recombination was likely to be common in this single-layer photovoltaic device [125].

SB Mdluli et al. discussed the application of π-conjugated polymers in organic and hybrid organic–silicon solar cells, focusing on the technical results and discussions. This review highlighted the use of carrier-selective layers on crystalline silicon wafers, achieving a record-breaking power conversion efficiency (PCE) of 26.6%. It delved into the electronic band structure, doping mechanisms, and role of π-conjugated polymers as hole transporting layers (HTLs), emphasizing their contribution to achieving low band gaps and superior electrical conductivity. This review also addressed the significance of the thickness of transparent conductive oxide (TCO) layers in solar cell applications, stressing the need to balance transmittance, sheet resistivity, and smooth morphologies. Additionally, the study discussed the impact of different morphologies of silicon substrates and nanostructures on solar cell performance, providing insights into strategies for enhancing the efficiency [126]. PTB7:PC70BM was used as the active layer in a unique polymer solar cell design by Alahmadi et al., who produced a maximum PCE of over 8%. The ideal doping density and layer thickness were determined by numerically simulating the solar cell operation. A Voc of 0.731 volts, FF of 68.055%, and Jsc of 16.434 mA/cm^2 were achieved by the optimized solar cell. Nonetheless, the experimental findings demonstrated that the doping density and layer thickness had a major impact on photovoltaic characteristics. This research also addressed how traps affect the overall photovoltaic response and proposed that the lower PCE observed in the simulations could have been caused by a larger density of traps [127].

5.4. Organic Phototransistors

As a significant development in optoelectronics, organic phototransistors (OPTs) can detect and amplify light signals using the unique characteristics of organic materials. These devices combine the advantages of traditional transistors and photodetectors to provide

increased sensitivity and adaptability for various applications. Organic semiconductors (OPTs) are composed of carbon-based materials recognized for their adaptability, low weight, and potential for large-scale, commercially successful production. The unique qualities of OPTs make them particularly appealing for a variety of cutting-edge applications including flexible electronics, biomedical devices, and environmental monitoring. An example of a standard design of an organic phototransistor is shown in Figure 15 [128,129].

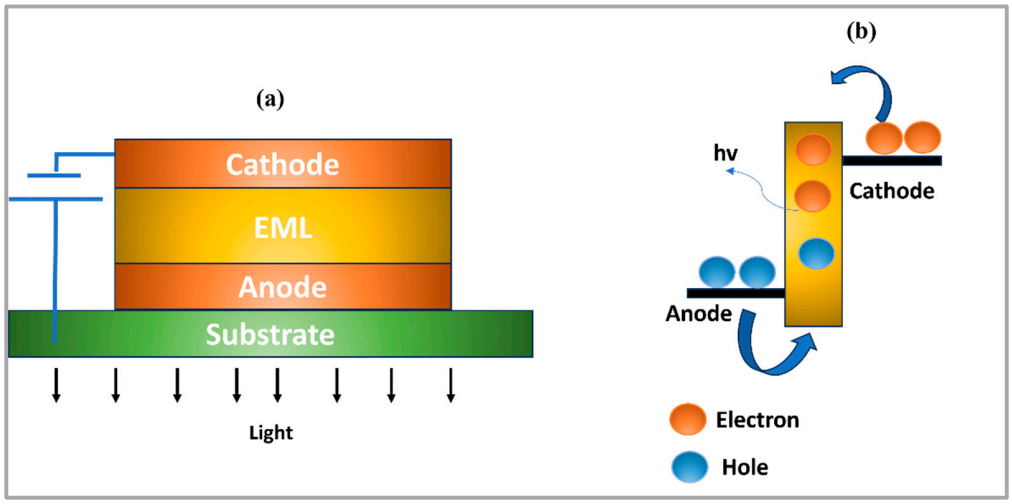

Figure 15. (**a**) Schematics, (**b**) energy band diagrams, and working mechanism of organic photo transistor [128].

5.4.1. Basic Principles and Structure

OPTs function by combining the characteristics of a photodetector and a transistor, allowing them to amplify electrical signals in response to light. An OPT is composed of three layers: the active organic semiconductor layer, which is situated between the source and drain electrodes, the dielectric, and the gate. The gate electrode delivers a voltage that regulates the current flow between the source and drain even though the dielectric layer shields the gate from the semiconductor layer. The active organic layer, which forms the OPT core, is where light absorption and photoinduced charge generation occur. The performance of the OPT as a whole, charge mobility, and light sensitivity are critically dependent on the organic semiconducting materials in this layer, which may be polymers or small molecules. Organic phototransistors (OPTs) are structurally similar to field-effect transistors (FETs), with the addition of light sensitivity caused by the organic semiconductors.

5.4.2. Working Mechanism

The ability of an organic phototransistor to separate charges, transfer charges, produce excitons, and absorb light are all essential processes. When light absorption causes electrons in an organic semiconductor to become excited and migrate from the valence band to the conduction band, pairs of electrons known as excitons are formed. It is necessary to separate these bound excitons into free charge carriers to produce photocurrents. After photon absorption, the excitons migrate to the organic semiconductor gate dielectric contact.

When the given gate voltage produced an internal electric field, the excitons began to split into free electrons and holes. A detectable photocurrent was then created when these free charge carriers moved to the source and drain electrodes. The gate voltage is crucial for regulating the mobility and density of charge carriers in the semiconductor layer, which is necessary for varying the current between the source and drain electrodes in response to lighting.

A phototransistor (p-OPT) with a hybrid gate insulator structure was created by Hea-Lim Park and colleagues in an effort to improve optical switching efficiency. A gate insulator consisting of two layers makes up this device: an interfacial layer of poly(methyl methacrylate)

(PMMA) prevents photogenerated minority carriers from being trapped, thereby ensuring reliable optical switching, and a photo-responsive layer of poly(4-vinylphenol) (PVP) improves the UV light responsiveness and offers excellent optical and dielectric properties.

Assessing the drain current as a function of time during UV light exposure allowed researchers to determine the real-time photo response of p-OPTs. According to Figure 16a,b, 5 s UV light exposure at 15 s intervals specifically demonstrated the dynamic photoresponsivity activity. The darkened regions in these figures depict the times of UV light exposure. Depending on the UV light, both p-OPTs exhibited a well-characterized optical switching behavior. Interestingly, the application of UV light caused the drain current to increase sharply, a behavior primarily caused by the creation of electron–hole pairs.

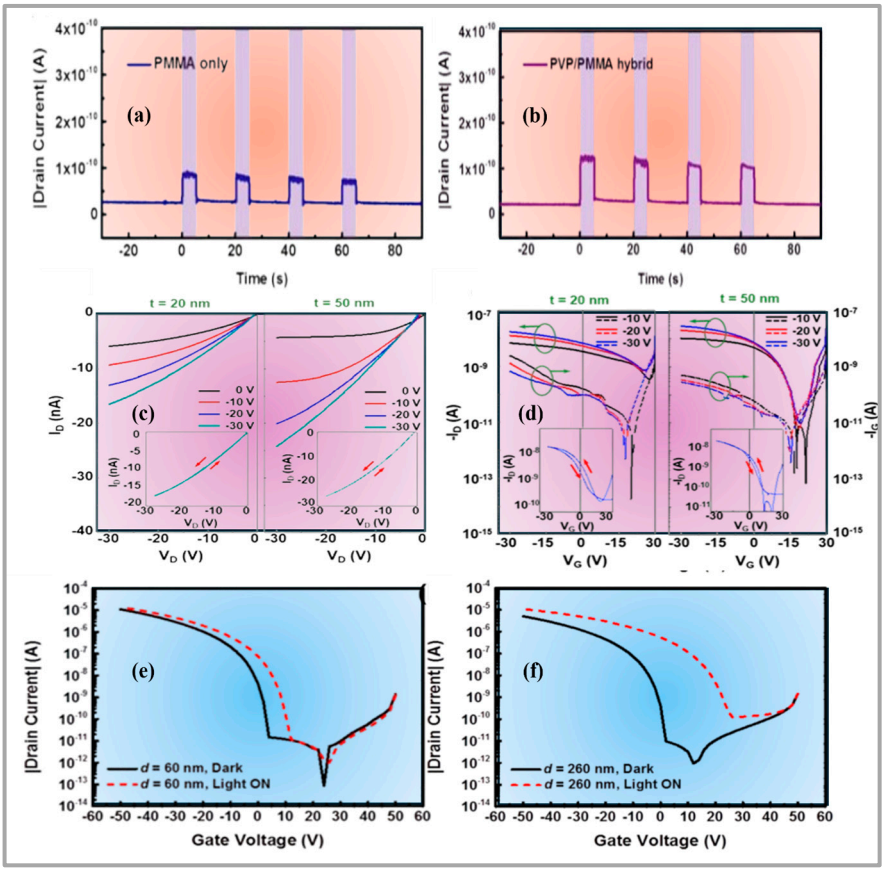

Figure 16. Dynamic photo-responsive behavior of organic field−effect transistors (OPTs) with (**a**) PMMA and (**b**) hybrid PVP/PMMA gate insulators under UV exposure. Output (**c**) and transfer (**d**) curves of NIR−OPTRs with varying PMMA thicknesses (t = 20 nm and t = 50 nm) in the dark. Insets (**e**,**f**) display output and transfer curves for different PVP thicknesses (d = 60 nm and d = 260 nm) under light and dark conditions [130–132].

Although the hole-trapping properties of PMMA-based organic field-effect transistors have been described, the number of trapped electrons and holes at the PMMA/organic semiconductor (OSC) interface was not very large. After the UV light was turned off, the drain current returned to its original value. In devices with a single-polymer insulator, the constant current levels under UV exposure were 7.98×10^{-11} A, whereas in devices with a hybrid gate insulator, they were 1.17×10^{-10} A. Consequently, the device utilizing the hybrid gate insulator exhibited a photo response that was 1.47 times greater than that of the reference device [130].

Kim et al. developed a Near-Infrared Optical Phototransistor (NIR-OPTR) featuring a polymeric channel/dielectric/sensing (CDS) structure configured in a bottom-gate bottom-source/drain contact transistor arrangement. This structure was constructed by sequential spin coating of poly(3-hexylthiophene) (P3HT), poly(methyl methacrylate) (PMMA),

and poly[{2,5-bis-(2-octyldodecyl)-3,6-bis-(thien-2-yl)-pyrrolo[3,4-c]pyrrole-1,4-di-co-{2,2′-(2,1] (PODTPPD-BT) onto PMMA gate-insulating layers deposited on silver electrodes. In this setup, the central PMMA dielectric layer plays a dual role: it not only protects the underlying channel layers during spin coating but also aids in dipole induction from photogenerated excitons.

Tests were conducted to assess the effect of two distinct PMMA dielectric layer thicknesses (20 nm and 50 nm) on the sensor's performance in terms of reflected NIR light detection and near-infrared (NIR) light modulation. To comprehend the fundamental transistor properties of CDS structures, measurements were made of the OPTRs' performance in the dark. At a given drain voltage (VD), the output curves (Figure 16c) show the characteristic behavior of the p-channel transistors, with the drain current (ID) clearly dependent on the gate voltage (VG). A significant difference was observed in the drain current between devices with PMMA dielectric layers that were 50 nm thick and those that had 20 nm thick. The transfer curves (Figure 16d) likewise show this pattern. The output curves showed very little hysteresis, whereas the transfer curves showed only a small amount of hysteresis, as shown by the dark sweeps. Moreover, the gate current (IG) measurements for each example showed that devices with 20 nm thick PMMA dielectric layers had noticeably worse off currents than those with 50 nm thick layers [131].

Park et al. synthesized an organic phototransistor (OPT) using silicon wafers as gate electrodes and a 300 nm thick SiO2 layer that was thermally generated as the first gate insulator. Poly(4-vinylphenol) (PVP) combined with poly(melamine-co-formaldehyde) was spin-coated at two weight percent and seven weight percent concentrations to obtain PVP layer thicknesses of approximately 60 nm and 260 nm for the second gate insulator, respectively. Next, the PVP layers were annealed at 100 and 200 °C. The PVP layers were covered with a 50 nm thick layer of pentacene, which was thermally evaporated. Next, using a shadow mask, gold (Au) was deposited to construct the source and drain electrodes, featuring 150 µm × 1 mm channel dimensions. Under ambient conditions, the electrical properties of the OPTs were evaluated using a semiconductor parameter analyzer and the photo response was determined at a peak wavelength of 365 nm using a UV light source. The transfer curves for the OPTs at a drain voltage (Vd) of −50 V and gate voltages (Vg) between 50 and −50 V are shown in Figure 16e,f. A mobility of around 0.16 cm^2/Vs was demonstrated by both devices, which had PVP layer thicknesses of 60 nm and 260 nm. The device with the thicker PVP layer had a more negative threshold voltage (Vth) of −8.4 V compared with the thinner layer's −7.4 V. This was because the thicker insulator had a lower capacitance of 5.41 nF/cm^2 than that of the thinner insulator, which had an 8.08 nF/cm^2 capacitance. Therefore, a higher bias was required to turn this on. Owing to the smaller gate insulator's greater capacitance, the OPT with the 60 nm PVP layer had a larger drain current at a given gate voltage Vg of 0 to −50 V (electrically on state) than the 260 nm device. For the 60 nm device, the on–off ratio values were 7.46 × 10^5, while for the 260 nm device, they were 5.20 × 10^5 [132].

Wang et al. used an inkjet printing method in conjunction with a direct solution-based patterning methodology to develop a novel three-dimensional (3D) channel structure for zinc-oxide (ZnO)-based thin-film transistors (TFTs). They achieved successful narrowing of the channel width by increasing the substrate temperature to hasten solution evaporation. Oxygen plasma treatment led to significant improvements in the stability and electrical properties. With the photocurrent produced by excited electron–hole pairs in the ZnO channel layer, the device demonstrated effective UV light detection. Voltage bias was applied to improve carrier migration, change energy bands, and improve channel conductivity, all of which contributed to the controlled amplification of the UV-induced photocarriers. The internal field in the photoactive layer effectively gathered photocarriers, which also increased the saturation current and allowed the electrical properties to recover without trapping the carriers. In addition, plasmon energy was detected using a metal–semiconductor junction structure, expanding the detection range from ultraviolet to visible light wavelengths. This work expands the development of large-area electronic devices suitable for UV and

visible light detection, as well as optoelectronics research, by highlighting the efficiency of the inkjet printing technique in producing 3D channel structures and illustrating how variations in channel morphology affect the electrical properties [133].

Moschetto employed a conjugated polar polymer (CPP) in a stacked arrangement to maximize the charge injection in multilayer organic light-emitting transistors (OLETs). Although CPPs show great promise, little is known about their functions in planar field-effect transistors. Multilayer OLETs with an emissive CPP (FBT-EP) and an electron-transporting semiconductor (DFH-4T) were the subjects of this study. Despite being designed to improve charge injection, the CPP layer prevented exciton generation in the emissive layer (EML). This was probably because the polarizability of CPP changed its LUMO level, which in turn changed the electrostatic potential profile. Owing to the possibility of CPP obstructing hole injection and decreasing source–drain current, the inclusion of both hole- and electron-transporting semiconductors in ambipolar multilayer OLETs introduces complications. It was highlighted that more research is necessary to investigate the fluctuations in CPP energy levels caused by polarization-induced dipoles; however, the movement of the charge recombination zone into FBT-EP was dismissed. Consequently, techniques for more effective ambipolar OLETs than OLEDs can be refined. Research also shows that incorporating CPPs into organic stacks makes it easier to examine charge- and field-induced processes [134].

6. Future Outlook and Challenges

Organic optoelectronic devices are poised for significant advancements in performance and efficiency, owing to continuous innovations in material synthesis, molecular engineering, and device architecture. The diagrammatic representation in Figure 17 outlines the anticipated future outlook for organic materials. It highlights the emerging trends, advancements, and potential research directions that are expected to shape the field. The power conversion efficiency (PCEs) of OSCs has surpassed 19%, while OLEDs now offer high brightness and excellent color purity, making them suitable for display and lighting applications [98,135]. The development of novel materials, including non-fullerene acceptors (NFAs) for OSCs and new emissive materials for OLEDs, is driving these efforts. Additionally, perovskite–organic hybrid structures are being explored for OPDs and OPTs, with promising enhancements in sensitivity, stability, and operational speed. Tandem and multijunction architectures, such as layered structures in OSCs, capture a broader spectrum of sunlight and significantly boost efficiency. Similarly, stacked OLEDs enhance brightness and expand color versatility [136]. The inherent flexibility of organic materials paves the way for innovative applications in wearable devices, foldable displays, and stretchable electronics, thereby opening new avenues in health monitoring, electronic skin, and wearable photodetectors.

Organic optoelectronic devices also benefit from cost-effective and scalable manufacturing, owing to the solution-processable nature of organic materials [137]. Techniques such as inkjet printing, roll-to-roll processing, and slot-die coating enable large-scale production at a fraction of the cost of traditional semiconductor fabrication, which is particularly advantageous for large-area applications, such as solar panels and displays [138,139]. Organic materials can be produced at lower temperatures, reducing energy consumption and minimizing the environmental impact compared with conventional silicon-based technologies. This eco-friendly aspect is becoming increasingly important as sustainability concerns increase [140]. Furthermore, organic materials offer customizable properties through molecular engineering, which allows designers to tailor their optical, electrical, and mechanical characteristics for specific applications. For example, OPDs can be designed to respond to a wide range of wavelengths from ultraviolet to near-infrared, making them suitable for imaging, environmental monitoring, and biomedical applications [141]. OLEDs are at the forefront of advanced display technologies because they provide superior contrast, faster response times, and lower power consumption than traditional LCDs. Future OLEDs could incorporate quantum dots or perovskite-based emitters to improve performance. High-

sensitivity organic phototransistors are also gaining traction owing to their low operating voltage, fast response, and potential in medical diagnostics, imaging, and communication technologies, highlighting the diverse and expanding role of organic optoelectronics in the future [142].

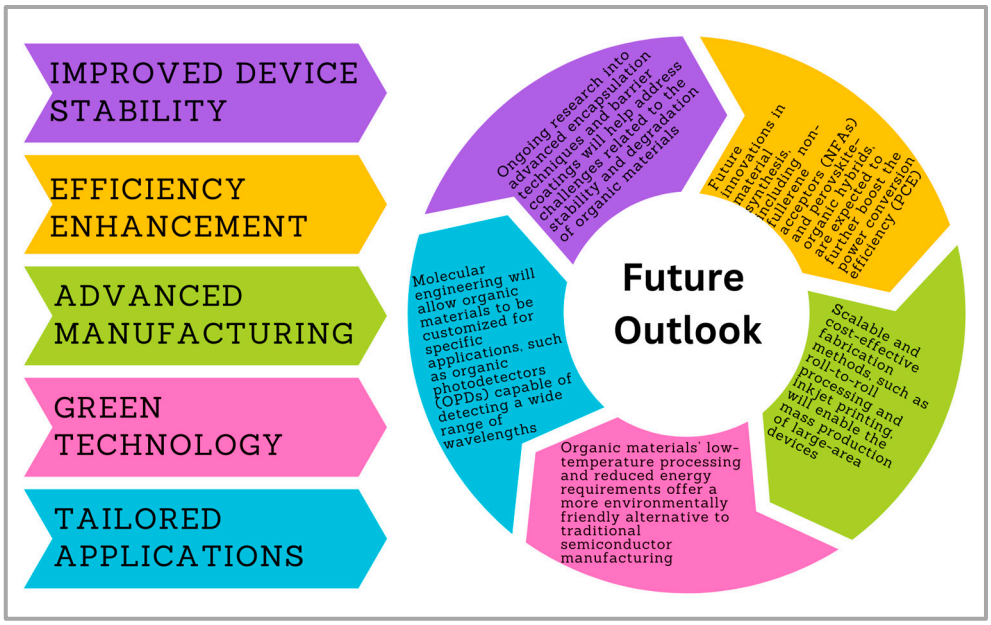

Figure 17. Illustration of future prospects for organic materials.

Despite this promising future, several challenges must be addressed to fully realize the potential of organic optoelectronic devices. One major issue is the stability and degradation of organic materials, which are prone to deterioration when exposed to environmental factors such as oxygen, moisture, and UV light, leading to reduced device lifetimes [143]. In devices such as organic solar cells (OSCs) and organic light-emitting diodes (OLEDs), prolonged exposure to light and oxygen can cause photooxidation and other chemical changes that degrade performance, resulting in efficiency losses and color shifts [144]. Developing effective encapsulation solutions, including advanced barrier coatings and encapsulation materials, is essential to protect organic devices from environmental degradation. However, achieving a long-term stability comparable to that of inorganic devices remains a significant challenge.

Another critical issue is the inherently low charge carrier mobility of organic materials compared with that of inorganic semiconductors such as silicon or gallium arsenide (GaAs). This limitation affects device efficiency, particularly in OSCs and organic phototransistors (OPTs), where poor charge transport and high recombination losses can significantly reduce the performance. Advanced interface engineering, including the use of interfacial layers and self-assembled monolayers, is crucial for minimizing recombination loss and enhancing charge extraction. Additionally, the presence of trap states and structural defects in organic materials often leads to inefficient charge transport, necessitating ongoing research to improve material purity and molecular design to minimize these defects. Scalability and uniformity in large-scale production also present significant challenges; achieving consistent film thickness, crystallinity, and phase separation across large areas remains challenging [145]. Techniques such as solution shearing, blade coating, and vapor deposition are being optimized to produce uniform films with high crystallinity; however, scaling these processes from lab to commercial production remains complex. Variations between material batches can also lead to inconsistent device performances, highlighting the need for stringent quality control during synthesis and processing.

The long-term operational stability of organic devices is not yet fully understood, particularly under real-world conditions involving temperature cycling, mechanical stress,

and prolonged light exposure [146]. Comprehensive aging studies are required to identify the key degradation pathways and develop strategies to mitigate them, which is crucial for applications requiring long-term reliability, such as outdoor solar panels and medical sensors. Predictive modeling using advanced computational tools can also aid in understanding material and device behavior under various conditions, guiding the design of more robust organic optoelectronic devices. Additionally, the environmental and health concerns associated with the use of toxic solvents, processing chemicals, and degradation products must be addressed. Developing green solvents and non-toxic materials is essential for sustainable production, and ensuring the safe disposal or recycling of organic devices at the end of their life cycle is critical for minimizing their environmental impact.

The future of organic materials in optoelectronics is promising, but challenges remain, particularly in terms of material stability, performance consistency, and device longevity. Organic materials tend to degrade under environmental stressors like oxygen and moisture, which impacts both OSCs and OLEDs. Additionally, issues such as reproducibility in synthesis and the scalability of fabrication techniques need to be addressed to ensure the widespread adoption of these materials in commercial devices. While these challenges are common across different devices, specific optimizations, such as enhancing stability for OSCs or improving color purity for OLEDs, will be crucial for advancing the field. Continued research into material design, synthesis optimization, and device architecture will be essential to overcome these obstacles.

7. Conclusions

This review of organic materials for next-generation optoelectronics underscores the remarkable progress and potential of these materials in revolutionizing the field of optoelectronics. The unique properties of organic materials, such as their light weight, flexibility, and simple processing, position them as key components in the development of advanced optoelectronic devices, including organic solar cells, thin-film transistors, and OLEDs. The study has shed light on the challenges associated with stability, scalability, and performance, emphasizing the need for further research and development to address these issues. Additionally, the review has highlighted the diverse electronic properties of organic materials, underscoring their critical role in enhancing the performance of optoelectronic devices. The comprehensive evaluation of the synthesis, properties, and applications of organic materials provides valuable insights into their potential and the opportunities they present for the future of optoelectronics. The review also emphasizes the importance of ongoing research to achieve consistent performance across various types of devices and to maximize the integration of organic materials into commercial products. This review serves as a catalyst for further exploration and innovation in leveraging organic materials for next-generation optoelectronics, paving the way for transformative advancements in the field.

Author Contributions: Conceptualization, G.A.N.; methodology, G.A.N.; writing—original draft preparation, G.A.N. and Q.A.; writing—review and editing, M.K., M.A. and U.F.A.; resources and funding acquisition, Q.A., G.A.N. and S.S.H.; and supervision, S.S.H. All authors have read and agreed to the published version of the manuscript.

Funding: This research received no external funding.

Data Availability Statement: All data generated or analyzed during this study are included in this published article.

Acknowledgments: The authors are grateful to Centre of Excellence in Solid State Physics, University of the Punjab, Lahore, for all the necessary support.

Conflicts of Interest: The authors declare no conflicts of interest.

References

1. Nguyen, T.P. *Defects in Organic Semiconductors and Devices*; John Wiley & Sons: Hoboken, NJ, USA, 2023.
2. Alvertis, A.M.; Alvertis, A.M. Organic Semiconductors and Their Properties. In *On Exciton–Vibration and Exciton–Photon Interactions in Organic Semiconductors*; Springer: Berlin/Heidelberg, Germany, 2021; pp. 7–23.
3. Shivaleela, B.; Hanagodimath, S. Organic Smart Materials: Synthesis, Characterization, and Application. In *Smart Materials for Science and Engineering*; John Wiley & Sons: Hoboken, NJ, USA, 2024; pp. 121–134.
4. Mir, S.H.; Nagahara, L.A.; Thundat, T.; Mokarian-Tabari, P.; Furukawa, H.; Khosla, A. Review—Organic-Inorganic Hybrid Functional Materials: An Integrated Platform for Applied Technologies. *J. Electrochem. Soc.* **2018**, *165*, B3137–B3156. [CrossRef]
5. Li, D.; Yu, J. Aiegens-functionalized inorganic-organic hybrid materials: Fabrications and applications. *Small* **2016**, *12*, 6478–6494. [CrossRef]
6. Mitzi, D.B.; Chondroudis, K.; Kagan, C.R. Organic-inorganic electronics. *IBM J. Res. Dev.* **2001**, *45*, 29–45. [CrossRef]
7. Feron, K.; Lim, R.; Sherwood, C.; Keynes, A.; Brichta, A.; Dastoor, P.C. Organic Bioelectronics: Materials and Biocompatibility. *Int. J. Mol. Sci.* **2018**, *19*, 2382. [CrossRef]
8. Liu, K.; Ouyang, B.; Guo, X.; Guo, Y.; Liu, Y. Advances in flexible organic field-effect transistors and their applications for flexible electronics. *npj Flex. Electron.* **2022**, *6*, 1–19. [CrossRef]
9. Root, S.E.; Savagatrup, S.; Printz, A.D.; Rodriquez, D.; Lipomi, D.J. Mechanical Properties of Organic Semiconductors for Stretchable, Highly Flexible, and Mechanically Robust Electronics. *Chem. Rev.* **2017**, *117*, 6467–6499. [CrossRef]
10. Wang, Y.; Sun, L.; Wang, C.; Yang, F.; Ren, X.; Zhang, X.; Dong, H.; Hu, W. Organic crystalline materials in flexible electronics. *Chem. Soc. Rev.* **2019**, *48*, 1492–1530. [CrossRef]
11. Boix, P.P.; Nonomura, K.; Mathews, N.; Mhaisalkar, S.G. Current progress and future perspectives for organic/inorganic perovskite solar cells. *Mater. Today* **2014**, *17*, 16–23. [CrossRef]
12. Liu, C. Organic Electronics: Material Innovations, Synthesis Strategies, and Applications as Flexible Electronics. *Highlights Sci. Eng. Technol.* **2024**, *106*, 332–337. [CrossRef]
13. Huang, Q.; Pan, B.; Wang, Z. Organic Electronics in Flexible Devices: Engineering Strategy, Synthesis, And Application. *Highlights Sci. Eng. Technol.* **2024**, *96*, 251–260. [CrossRef]
14. Kong, D.; Lv, W.; Liu, R.; He, Y.-B.; Wu, D.; Li, F.; Fu, R.; Yang, Q.-H.; Kang, F. Superstructured carbon materials: Design and energy applications. *Energy Mater. Devices* **2023**, *1*, 9370017. [CrossRef]
15. Gomes Ferreira de Paula, F.; Campello-Gómez, I.; Ortega, P.F.R.; Rodríguez-Reinoso, F.; Martínez-Escandell, M.; Silvestre-Albero, J. Structural flexibility in activated carbon materials prepared under harsh activation conditions. *Materials* **2019**, *12*, 1988. [CrossRef] [PubMed]
16. Xie, G.; Xiao, D.; Yang, Q.; Ye, T.; Chen, R.; Huang, W. Luminescent organic radicals toward breakthrough of organic optoelectronics. In *Organic Radicals*; Elsevier: Amsterdam, The Netherlands, 2024; pp. 183–209.
17. Yang, Y.; Wu, Y.; Bin, Z.; Zhang, C.; Tan, G.; You, J. Discovery of Organic Optoelectronic Materials Powered by Oxidative Ar–H/Ar–H Coupling. *J. Am. Chem. Soc.* **2024**, *146*, 1224–1243. [CrossRef]
18. Ravikumar, K.; Dangate, M.S. Advancements in Stretchable Organic Optoelectronic Devices and Flexible Transparent Conducting Electrodes: Current Progress and Future Prospects. *Heliyon* **2024**, *10*, e33002. [CrossRef] [PubMed]
19. Ma, X. Applications of Two-Dimensional Organic Materials in the Field of Optoelectronics. *Highlights Sci. Eng. Technol.* **2024**, *87*, 167–172. [CrossRef]
20. Ostroverkhova, O. Organic optoelectronic materials: Mechanisms and applications. *Chem. Rev.* **2016**, *116*, 13279–13412. [CrossRef] [PubMed]
21. Lee, K.; Wan, Y.; Huang, Z.; Zhao, Q.; Li, S.; Lee, C. Organic optoelectronic materials: A rising star of bioimaging and phototherapy. *Adv. Mater.* **2024**, *36*, 2306492. [CrossRef]
22. Islam, A.; Usman, K.; Haider, Z.; Alam, M.F.; Nawaz, A.; Sonar, P. Biomass-Derived Materials for Interface Engineering in Organic/Perovskite Photovoltaic and Light-Emitting Devices. *Adv. Mater. Technol.* **2023**, *8*, 2201390. [CrossRef]
23. Choy, W.C.; Chan, W.K.; Yuan, Y. Recent advances in transition metal complexes and light-management engineering in organic optoelectronic devices. *Adv. Mater.* **2014**, *26*, 5368–5399. [CrossRef]
24. Baeg, K.-J.; Binda, M.; Natali, D.; Caironi, M.; Noh, Y.-Y. Organic light detectors: Photodiodes and phototransistors. *Adv. Mater.* **2013**, *25*, 4267–4295. [CrossRef]
25. Xie, C.; You, P.; Liu, Z.; Li, L.; Yan, F. Ultrasensitive broadband phototransistors based on perovskite/organic-semiconductor vertical heterojunctions. *Light. Sci. Appl.* **2017**, *6*, e17023. [CrossRef] [PubMed]
26. Xie, C.; Liu, C.K.; Loi, H.L.; Yan, F. Perovskite-based phototransistors and hybrid photodetectors. *Adv. Funct. Mater.* **2020**, *30*, 1903907. [CrossRef]
27. Zhao, Y.; Zhu, K. Organic–inorganic hybrid lead halide perovskites for optoelectronic and electronic applications. *Chem. Soc. Rev.* **2016**, *45*, 655–689. [CrossRef] [PubMed]
28. Bettinger, C.J.; Bao, Z. Organic thin film transistors fabricated on resorbable biomaterial substrates. *Adv. Mater.* **2010**, *22*, 651. [CrossRef]
29. Wang, G.-J.N.; Molina-Lopez, F.; Zhang, H.; Xu, J.; Wu, H.-C.; Lopez, J.; Shaw, L.; Mun, J.; Zhang, Q.; Wang, S.; et al. Nonhalogenated solvent processable and printable high-performance polymer semiconductor enabled by isomeric nonconjugated flexible linkers. *Macromolecules* **2018**, *51*, 4976–4985. [CrossRef]

30. Liu, H.; Liu, D.; Yang, J.; Gao, H.; Wu, Y. Flexible electronics based on organic semiconductors: From patterned assembly to integrated applications. *Small* **2023**, *19*, 2206938. [CrossRef]
31. Lee, E.K.; Lee, M.Y.; Park, C.H.; Lee, H.R.; Oh, J.H. Toward environmentally robust organic electronics: Approaches and applications. *Adv. Mater.* **2017**, *29*, 1703638. [CrossRef] [PubMed]
32. Rogge, S.M.; Waroquier, M.; Van Speybroeck, V. Reliably modeling the mechanical stability of rigid and flexible metal–organic frameworks. *Acc. Chem. Res.* **2018**, *51*, 138–148. [CrossRef]
33. He, T.; Kong, X.-J.; Li, J.-R. Chemically stable metal–organic frameworks: Rational construction and application expansion. *Acc. Chem. Res.* **2021**, *54*, 3083–3094. [CrossRef]
34. Chen, Z.; Li, Y.; Huang, F. Persistent and stable organic radicals: Design, synthesis, and applications. *Chem* **2021**, *7*, 288–332. [CrossRef]
35. Aguila, B.; Sun, Q.; Perman, J.A.; Earl, L.D.; Abney, C.W.; Elzein, R.; Schlaf, R.; Ma, S. Efficient mercury capture using functionalized porous organic polymer. *Adv. Mater.* **2017**, *29*, 1700665. [CrossRef] [PubMed]
36. Raimundo, J.M.; Garo, J.; Nicolini, T.; Sotiropoulos, J.M. Tunning the electronic properties of bridged dithienyl-, difuryl-, dipyrrolyl-vinylene as precursors of small bandgap conjugated polymers. *Chem. Eur. J.* **2024**, *30*, e202402461.
37. Wu, J.; Li, Q.; Wang, W.; Chen, K. Optoelectronic Properties and Structural Modification of Conjugated Polymers Based on Benzodithiophene Groups. *Mini-Rev. Org. Chem.* **2019**, *16*, 253–260. [CrossRef]
38. Zhang, C.; Guo, C.; Li, M.; Liu, H.; Han, L. Solution Processable Zn-Salphen Containing π-Conjugated Polymers with Unique Aggregation Behavior as Novel Organic Optoelectronic Materials. *J. Organomet. Chem.* **2024**, *1015*, 123232. [CrossRef]
39. Wang, H.; Yang, Y.; Zhang, Y.; Wang, S.; Tan, Z.; Yan, S.; Wang, L.; Hou, J.; Xu, B. p—π Conjugated Polyelectrolytes Toward Universal Electrode Interlayer Materials for Diverse Optoelectronic Devices. *Adv. Funct. Mater.* **2023**, *33*, 2213914. [CrossRef]
40. Cheng, Y.; Yao, H.-Q.; Zhang, Y.-D.; Shi, C.; Ye, H.-Y.; Wang, N. Nitrate-bridged hybrid organic-inorganic perovskites. *Chin. J. Struct. Chem.* **2024**, *43*, 100358. [CrossRef]
41. Feng, S.; Li, B.; Xu, B.; Wang, Z. Hybrid perovskites and 2D materials in optoelectronic and photocatalytic applications. *Crystals* **2023**, *13*, 1566. [CrossRef]
42. Dou, L. Organic semiconductor-incorporated perovskite (OSiP) lighting-emitting materials and devices (Conference Presentation). In *Organic and Hybrid Light Emitting Materials and Devices XXVI*; SPIE: Bellingham, WA, USA, 2022.
43. Luo, A.; Bao, Y.; Liu, J.; Yang, Y.; Deng, Y.; You, J.; Bin, Z. Design of Thermally Activated Delayed Fluorescence Materials: Transition from Carbonyl to Amide-Based Acceptor. *Angew. Chem. Int. Ed.* **2024**, *63*, e202411464.
44. Ferraro, V.; Bizzarri, C.; Bräse, S. Thermally Activated Delayed Fluorescence (TADF) Materials Based on Earth-Abundant Transition Metal Complexes: Synthesis, Design and Applications. *Adv. Sci.* **2024**, *11*, 2404866. [CrossRef]
45. Yuan, L.; Xu, J.W.; Yan, Z.P.; Yang, Y.F.; Mao, D.; Hu, J.J.; Ni, H.X.; Li, C.H.; Zuo, J.L.; Zheng, Y.X. Tetraborated Intrinsically Axial Chiral Multi-resonance Thermally Activated Delayed Fluorescence Materials. *Angew. Chem. Int. Ed.* **2024**, *63*, e202407277. [CrossRef]
46. Bang, J.; Jang, M.; Ahn, Y.; Park, C.W.; Nam, S.H.; Macdonald, J.; Cho, K.; Noh, Y.; Kim, Y.; Kim, Y.-H.; et al. Remotely Modulating the Optical Properties of Organic Charge-Transfer Crystallites via Molecular Packing. *J. Phys. Chem. Lett.* **2024**, *15*, 8676–8681. [CrossRef] [PubMed]
47. Kalita, K.J.; Vijayaraghavan, R.K. Organic charge transfer complex towards functional optical materials. *CrystEngComm* **2024**, *26*, 4751–4765. [CrossRef]
48. Huang, G. [Retracted] Organic Photoelectric Materials and Organic Photoelectric Devices Based on Smart Image Sensors. *Adv. Mater. Sci. Eng.* **2022**, *2022*, 4249657. [CrossRef]
49. Feng, L.; Li, Z.; Liu, Y.; Hua, L.; Wei, Z.; Cheng, Y.; Zhang, Z.; Xu, B. Counterion Engineering toward High-Performance and pH-Neutral Polyoxometalates-Based Hole-Transporting Materials for Efficient Organic Optoelectronic Devices. *ACS Nano* **2024**, *18*, 3276–3285. [CrossRef]
50. Li, Q.; Li, Z.; Liu, Y.; Zhang, Z.; Xu, B.; Yan, S. Mutual doping of conjugated polyelectrolytes and polyoxometalate towards high-performance hole transporting materials for organic optoelectronic devices. *Chem. Eng. J.* **2024**, *494*, 153008. [CrossRef]
51. Yang, Y.; Xu, B.; Hou, J. Mixed-Addenda Dawson-type polyoxometalates as high-performance anode interlayer materials for efficient organic optoelectronic devices. *Adv. Energy Mater.* **2023**, *13*, 2204228. [CrossRef]
52. Liao, C.; Zhang, M.; Yao, M.Y.; Hua, T.; Li, L.; Yan, F. Flexible organic electronics in biology: Materials and devices. *Adv. Mater.* **2015**, *27*, 7493–7527. [CrossRef]
53. Zhao, Y.S.; Fu, H.; Peng, A.; Ma, Y.; Liao, Q.; Yao, J. Construction and optoelectronic properties of organic one-dimensional nanostructures. *Acc. Chem. Res.* **2010**, *43*, 409–418. [CrossRef]
54. Lee, H.; Jiang, Z.; Yokota, T.; Fukuda, K.; Park, S.; Someya, T. Stretchable organic optoelectronic devices: Design of materials, structures, and applications. *Mater. Sci. Eng. R Rep.* **2021**, *146*, 100631. [CrossRef]
55. Zhugayevych, A.; Tretiak, S. Theoretical description of structural and electronic properties of organic photovoltaic materials. *Annu. Rev. Phys. Chem.* **2015**, *66*, 305–330. [CrossRef]
56. Rajagopal, A.; Wu, C.; Kahn, A. Energy level offset at organic semiconductor heterojunctions. *J. Appl. Phys.* **1998**, *83*, 2649–2655. [CrossRef]
57. Kroon, R.; Lenes, M.; Hummelen, J.C.; Blom, P.W.M.; de Boer, B. Small bandgap polymers for organic solar cells (polymer material development in the last 5 years). *Polym. Rev.* **2008**, *48*, 531–582. [CrossRef]

58. Stehr, V.; Pfister, J.; Fink, R.F.; Engels, B.; Deibel, C. First-principles calculations of anisotropic charge-carrier mobilities in organic semiconductor crystals. *Phys. Rev. B-Condens. Matter Mater. Phys.* **2011**, *83*, 155208. [CrossRef]
59. Xie, L.S.; Skorupskii, G.; Dinca, M. Electrically conductive metal–organic frameworks. *Chem. Rev.* **2020**, *120*, 8536–8580. [CrossRef] [PubMed]
60. Daliento, S.; Tari, O.; Lancellotti, L. Closed-form analytical expression for the conductive and dissipative parameters of the MOS-C equivalent circuit. *IEEE Trans. Electron Devices* **2011**, *58*, 3643–3646. [CrossRef]
61. Haneef, H.F.; Zeidell, A.M.; Jurchescu, O.D. Charge carrier traps in organic semiconductors: A review on the underlying physics and impact on electronic devices. *J. Mater. Chem. C* **2020**, *8*, 759–787. [CrossRef]
62. Chen, J.; Yang, J.; Guo, Y.; Liu, Y. Acceptor Modulation Strategies for Improving the Electron Transport in High-Performance Organic Field-Effect Transistors. *Adv. Mater.* **2022**, *34*, 2104325. [CrossRef] [PubMed]
63. Tang, M.; Zhu, S.; Liu, Z.; Jiang, C.; Wu, Y.; Li, H.; Wang, B.; Wang, E.; Ma, J.; Wang, C. Tailoring π-conjugated systems: From π-π stacking to high-rate-performance organic cathodes. *Chem* **2018**, *4*, 2600–2614. [CrossRef]
64. Schröter, M.; Ivanov, S.; Schulze, J.; Polyutov, S.; Yan, Y.; Pullerits, T.; Kühn, O. Exciton–vibrational coupling in the dynamics and spectroscopy of Frenkel excitons in molecular aggregates. *Phys. Rep.* **2015**, *567*, 1–78. [CrossRef]
65. Nivaz, S.R.; Geethalakshmi, R.; Lekshmi, G.S.; Surendhiran, D.; Hussain, C.M.; Sirajunnisa, A.R. Utilization of Raman spectroscopy in nanomaterial/bionanomaterial detection. In *Handbook of Microbial Nanotechnology*; Academic Press: Cambridge, MA, USA, 2022; pp. 145–156.
66. Xie, L.; Zhang, J.; Song, W.; Hong, L.; Ge, J.; Wen, P.; Tang, B.; Wu, T.; Zhang, X.; Li, Y.; et al. Understanding the Effect of Sequential Deposition Processing for High-Efficient Organic Photovoltaics to Harvest Sunlight and Artificial Light. *ACS Appl. Mater. Interfaces* **2021**, *13*, 20405–20416. [CrossRef]
67. Schnabel, W. *Polymers and Light: Fundamentals and Technical Applications*; John Wiley & Sons: Hoboken, NJ, USA, 2007.
68. Steinberg, I.Z. Long-Range Nonradiative Transfer of Electronic Excitation Energy in Proteins and Polypeptides. *Annu. Rev. Biochem.* **1971**, *40*, 83–114. [CrossRef] [PubMed]
69. Mazumder, M.R.H.; Mathews, L.D.; Mateti, S.; Salim, N.V.; Parameswaranpillai, J.; Govindaraj, P.; Hameed, N. Boron nitride based polymer nanocomposites for heat dissipation and thermal management applications. *Appl. Mater. Today* **2022**, *29*, 101672. [CrossRef]
70. Jang, Y.J.; Chung, K.; Lee, J.S.; Choi, C.H.; Lim, J.W.; Kim, D.H. Plasmonic Hot Carriers Imaging: Promise and Outlook. *ACS Photonics* **2018**, *5*, 4711–4723. [CrossRef]
71. Tilchin, J.; Dirin, D.N.; Maikov, G.I.; Sashchiuk, A.; Kovalenko, M.V.; Lifshitz, E. Hydrogen-like Wannier–Mott Excitons in Single Crystal of Methylammonium Lead Bromide Perovskite. *ACS Nano* **2016**, *10*, 6363–6371. [CrossRef]
72. Chen, X.-K.; Kim, D.; Brédas, J.-L. Thermally Activated Delayed Fluorescence (TADF) Path toward Efficient Electroluminescence in Purely Organic Materials: Molecular Level Insight. *Accounts Chem. Res.* **2018**, *51*, 2215–2224. [CrossRef]
73. Wang, T.; Wang, M.; Fu, L.; Duan, Z.; Chen, Y.; Hou, X.; Wu, Y.; Li, S.; Guo, L.; Kang, R.; et al. Enhanced Thermal Conductivity of Polyimide Composites with Boron Nitride Nanosheets. *Sci. Rep.* **2018**, *8*, 1557. [CrossRef]
74. Yi, M.; Shen, Z. A review on mechanical exfoliation for the scalable production of graphene. *J. Mater. Chem. A* **2015**, *3*, 11700–11715. [CrossRef]
75. Le, T.; Oh, Y.; Kim, H.; Yoon, H. Exfoliation of 2D Materials for Energy and Environmental Applications. *Chem. Eur. J.* **2020**, *26*, 6360–6401. [CrossRef] [PubMed]
76. Zhang, X.; Chen, X.; Chen, T.; Ma, G.; Zhang, W.; Huang, L. Influence of Pulse Energy and Defocus Amount on the Mechanism and Surface Characteristics of Femtosecond Laser Polishing of SiC Ceramics. *Micromachines* **2022**, *13*, 1118. [CrossRef]
77. Tamaki, Y.; Asahi, T.; Masuhara, H. Nanoparticle Formation of Vanadyl Phthalocyanine by Laser Ablation of Its Crystalline Powder in a Poor Solvent. *J. Phys. Chem. A* **2002**, *106*, 2135–2139. [CrossRef]
78. Asahi, T.; Sugiyama, T.; Masuhara, H. Laser Fabrication and Spectroscopy of Organic Nanoparticles. *Accounts Chem. Res.* **2008**, *41*, 1790–1798. [CrossRef] [PubMed]
79. Cao, Y.; Xiao, W.; Shen, G.; Ji, G.; Zhang, Y.; Gao, C.; Han, L. Carbonization and ball milling on the enhancement of Pb(II) adsorption by wheat straw: Competitive effects of ion exchange and precipitation. *Bioresour. Technol.* **2019**, *273*, 70–76. [CrossRef] [PubMed]
80. Wei, L.K.; Rahim, S.Z.A.; Abdullah, M.M.A.B.; Yin, A.T.M.; Ghazali, M.F.; Omar, M.F.; Nemeș, O.; Sandu, A.V.; Vizureanu, P.; Abdellah, A.E.-H. Producing Metal Powder from Machining Chips Using Ball Milling Process: A Review. *Materials* **2023**, *16*, 4635. [CrossRef] [PubMed]
81. Roy, K.; Sahoo, S.; Saha, A.; Adak, L. Ball Milling in Organic Transformations. *Curr. Org. Chem.* **2023**, *27*, 153–165. [CrossRef]
82. Obst, M.; Gasser, P.; Mavrocordatos, D.; Dittrich, M. TEM-specimen preparation of cell/mineral interfaces by Focused Ion Beam milling. *Am. Miner.* **2005**, *90*, 1270–1277. [CrossRef]
83. Bassim, N.; Scott, K.; Giannuzzi, L.A. Recent advances in focused ion beam technology and applications. *MRS Bull.* **2014**, *39*, 317–325. [CrossRef]
84. Manoccio, M.; Esposito, M.; Passaseo, A.; Cuscunà, M.; Tasco, V. Focused Ion Beam Processing for 3D Chiral Photonics Nanostructures. *Micromachines* **2020**, *12*, 6. [CrossRef]
85. Cominos, V.; Gavriilidis, A. An Experimental Study of Non-Uniform Pd Catalytic Monoliths. *Chem. Eng. Res. Des.* **2001**, *79*, 795–798. [CrossRef]

86. Keränen, J.; Carniti, P.; Gervasini, A.; Iiskola, E.; Auroux, A.; Niinistö, L. Preparation by atomic layer deposition and characterization of active sites in nanodispersed vanadia/titania/silica catalysts. *Catal. Today* **2004**, *91*, 67–71. [CrossRef]
87. Saeed, M.; Alshammari, Y.; Majeed, S.A.; Al-Nasrallah, E. Chemical Vapour Deposition of Graphene—Synthesis, Characterisation, and Applications: A Review. *Molecules* **2020**, *25*, 3856. [CrossRef]
88. Tao, Y.; Pescarmona, P.P. Nanostructured Oxides Synthesised via $scCO_2$-Assisted Sol-Gel Methods and Their Application in Catalysis. *Catalysts* **2018**, *8*, 212. [CrossRef]
89. Niederberger, M.; Pinna, N. *Metal Oxide Nanoparticles in Organic Solvents: Synthesis, Formation, Assembly and Application*; Springer Science & Business Media: Berlin/Heidelberg, Germany, 2009.
90. Feinle, A.; Elsaesser, M.S.; Hüsing, N. Sol–gel synthesis of monolithic materials with hierarchical porosity. *Chem. Soc. Rev.* **2016**, *45*, 3377–3399. [CrossRef] [PubMed]
91. Liu, Q.; He, P.; Yu, H.; Gu, L.; Ni, B.; Wang, D.; Wang, X. Single molecule–mediated assembly of polyoxometalate single-cluster rings and their three-dimensional superstructures. *Sci. Adv.* **2019**, *5*, eaax1081. [CrossRef]
92. Whitesides, G.M.; Mathias, J.P.; Seto, C.T. Molecular Self-Assembly and Nanochemistry: A Chemical Strategy for the Synthesis of Nanostructures. *Science* **1991**, *254*, 1312–1319. [CrossRef] [PubMed]
93. Rahe, P.; Nimmrich, M.; Kühnle, A. Substrate Templating upon Self-Assembly of Hydrogen-Bonded Molecular Networks on an Insulating Surface. *Small* **2012**, *8*, 2969–2977. [CrossRef]
94. Al-Kutubi, H.; Gascon, J.; Sudhölter, E.J.R.; Rassaei, L. Electrosynthesis of Metal–Organic Frameworks: Challenges and Opportunities. *ChemElectroChem* **2015**, *2*, 462–474. [CrossRef]
95. Salahandish, R.; Ghaffarinejad, A.; Naghib, S.M.; Niyazi, A.; Majidzadeh-A, K.; Janmaleki, M.; Sanati-Nezhad, A. Sandwich-structured nanoparticles-grafted functionalized graphene based 3D nanocomposites for high-performance biosensors to detect ascorbic acid biomolecule. *Sci. Rep.* **2019**, *9*, 1226. [CrossRef]
96. Hartmann, M.; Kunz, S.; Himsl, D.; Tangermann, O.; Ernst, S.; Wagener, A. Adsorptive separation of isobutene and isobutane on Cu3 (BTC) 2. *Langmuir* **2008**, *24*, 8634–8642. [CrossRef]
97. Tang, C.W.; Vanslyke, S.A. Organic electroluminescent diodes. *Appl. Phys. Lett.* **1987**, *51*, 913. [CrossRef]
98. Wei, Q.; Fei, N.; Islam, A.; Lei, T.; Hong, L.; Peng, R.; Fan, X.; Chen, L.; Gao, P.; Ge, Z. Small-molecule emitters with high quantum efficiency: Mechanisms, structures, and applications in OLED devices. *Adv. Opt. Mater.* **2018**, *6*, 1800512. [CrossRef]
99. Bauri, J.; Choudhary, R.B.; Mandal, G. Recent advances in efficient emissive materials-based OLED applications: A review. *J. Mater. Sci.* **2021**, *56*, 18837–18866. [CrossRef]
100. Zou, S.-J.; Shen, Y.; Xie, F.-M.; Chen, J.-D.; Li, Y.-Q.; Tang, J.-X. Recent advances in organic light-emitting diodes: Toward smart lighting and displays. *Mater. Chem. Front.* **2019**, *4*, 788–820. [CrossRef]
101. Lim, J.W. Polymer Materials for Optoelectronics and Energy Applications. *Materials* **2024**, *17*, 3698. [CrossRef] [PubMed]
102. Walzer, K.; Maennig, B.; Pfeiffer, M.; Leo, K. Highly efficient organic devices based on electrically doped transport layers. *Chem. Rev.* **2007**, *107*, 1233–1271. [CrossRef]
103. Amruth, C.; Pahlevani, M.; Welch, G.C. Organic light emitting diodes (OLEDs) with slot-die coated functional layers. *Mater. Adv.* **2021**, *2*, 628–645.
104. Teixeira, F.; Germino, J.C.; Pereira, L. Wet-Deposited TADF-Based OLED Active Layers: New Approaches towards Further Optimization. *Appl. Sci.* **2023**, *13*, 12020. [CrossRef]
105. Tavgeniene, D.; Zhang, B.; Grigalevicius, S. Di (arylcarbazole) substituted oxetanes as efficient hole transporting materials with high thermal and morphological stability for OLEDs. *Molecules* **2023**, *28*, 2282. [CrossRef]
106. Krucaite, G.; Tavgeniene, D.; Blazevicius, D.; Zhang, B.; Vembris, A.; Grigalevicius, S. New Electroactive Polymers with Electronically Isolated 4,7-Diarylfluorene Chromophores as Positive Charge Transporting Layer Materials for OLEDs. *Molecules* **2021**, *26*, 1936. [CrossRef]
107. De Silva, T.P.D.; Youm, S.G.; Fronczek, F.R.; Sahasrabudhe, G.; Nesterov, E.E.; Warner, I.M. Pyrene-benzimidazole derivatives as novel blue emitters for OLEDs. *Molecules* **2021**, *26*, 6523. [CrossRef]
108. Starykov, H.; Bezvikonnyi, O.; Leitonas, K.; Simokaitiene, J.; Volyniuk, D.; Skuodis, E.; Keruckiene, R.; Grazulevicius, J.V. Derivatives of Phenyl Pyrimidine and of the Different Donor Moieties as Emitters for OLEDs. *Materials* **2024**, *17*, 1357. [CrossRef]
109. Anabestani, H.; Nabavi, S.; Bhadra, S. Advances in Flexible Organic Photodetectors: Materials and Applications. *Nanomaterials* **2022**, *12*, 3775. [CrossRef] [PubMed]
110. Wang, H.; Lim, J.W.; Na Quan, L.; Chung, K.; Jang, Y.J.; Ma, Y.; Kim, D.H. Perovskite–Gold Nanorod Hybrid Photodetector with High Responsivity and Low Driving Voltage. *Adv. Opt. Mater.* **2018**, *6*, 1701397. [CrossRef]
111. Sze, S.M. *Semiconductor Devices: Physics and Technology*; John Wiley & Sons: Hoboken, NJ, USA, 2008.
112. Wang, H.; Lim, J.W.; Mota, F.M.; Jang, Y.J.; Yoon, M.; Kim, H.; Hu, W.; Noh, Y.-Y.; Kim, D.H. Plasmon-mediated wavelength-selective enhanced photoresponse in polymer photodetectors. *J. Mater. Chem. C* **2017**, *5*, 399–407. [CrossRef]
113. Lim, J.W.; Wang, H.; Choi, C.H.; Kwon, H.; Na Quan, L.; Park, W.-T.; Noh, Y.-Y.; Kim, D.H. Self-powered reduced-dimensionality perovskite photodiodes with controlled crystalline phase and improved stability. *Nano Energy* **2019**, *57*, 761–770. [CrossRef]
114. Yu, Y.-Y.; Peng, Y.-C.; Chiu, Y.-C.; Liu, S.-J.; Chen, C.-P. Realizing Broadband NIR Photodetection and Ultrahigh Responsivity with Ternary Blend Organic Photodetector. *Nanomaterials* **2022**, *12*, 1378. [CrossRef]
115. Zhai, A.; Zhao, C.; Pan, D.; Zhu, S.; Wang, W.; Ji, T.; Li, G.; Wen, R.; Zhang, Y.; Hao, Y.; et al. Organic Photodetectors with Extended Spectral Response Range Assisted by Plasmonic Hot-Electron Injection. *Nanomaterials* **2022**, *12*, 3084. [CrossRef]

116. Salem, M.S.; Shaker, A.; Al-Bagawia, A.H.; Aleid, G.M.; Othman, M.S.; Alshammari, M.T.; Fedawy, M. Narrowband Near-Infrared Perovskite/Organic Photodetector: TCAD Numerical Simulation. *Crystals* **2022**, *12*, 1033. [CrossRef]
117. Alwi, S.A.K.; Hisamuddin, S.N.; Abdullah, S.M.; Anuar, A.; Rahim, A.H.A.; Majid, S.R.; Bawazeer, T.M.; Alsoufi, M.S.; Alsenany, N.; Supangat, A. Naphthalocyanine-based NIR organic photodiode: Understanding the role of different types of fullerenes. *Micromachines* **2021**, *12*, 1383. [CrossRef]
118. Kumaresan, P.; Vegiraju, S.; Ezhumalai, Y.; Yau, S.L.; Kim, C.; Lee, W.-H.; Chen, M.-C. Fused-Thiophene Based Materials for Organic Photovoltaics and Dye-Sensitized Solar Cells. *Polymers* **2014**, *6*, 2645–2669. [CrossRef]
119. Hoppe, H.; Sariciftci, N.S. Organic solar cells: An overview. *J. Mater. Res.* **2004**, *19*, 1924–1945. [CrossRef]
120. Oh, Y.; Lim, J.W.; Kim, J.G.; Wang, H.; Kang, B.-H.; Park, Y.W.; Kim, H.; Jang, Y.J.; Kim, J.; Kim, D.H.; et al. Plasmonic periodic nanodot arrays via laser interference lithography for organic photovoltaic cells with >10% efficiency. *ACS Nano* **2016**, *10*, 10143–10151. [CrossRef] [PubMed]
121. Markvart, T.; Castañer, L. *Practical Handbook of Photovoltaics: Fundamentals and Applications*; Elsevier: Amsterdam, The Netherlands, 2003.
122. Revoju, S.; Biswas, S.; Eliasson, B.; Sharma, G.D. Phenothiazine-based small molecules for bulk heterojunction organic solar cells; variation of side-chain polarity and length of conjugated system. *Org. Electron.* **2019**, *65*, 232–242. [CrossRef]
123. Bangash, K.A.; Kazmi, S.A.A.; Farooq, W.; Ayub, S.; Musarat, M.A.; Alaloul, W.S.; Javed, M.F.; Mosavi, A. Thickness Optimization of Thin-Film Tandem Organic Solar Cell. *Micromachines* **2021**, *12*, 518. [CrossRef]
124. Nowsherwan, G.A.; Samad, A.; Iqbal, M.A.; Mushtaq, T.; Hussain, A.; Malik, M.; Haider, S.; Pham, P.V.; Choi, J.R. Performance analysis and optimization of a PBDB-T: ITIC based organic solar cell using graphene oxide as the hole transport layer. *Nanomaterials* **2022**, *12*, 1767. [CrossRef]
125. Islam, Z.U.; Tahir, M.; Syed, W.A.; Aziz, F.; Wahab, F.; Said, S.M.; Sarker, M.R.; Ali, S.H.M.; Sabri, M.F.M. Fabrication and photovoltaic properties of organic solar cell based on zinc phthalocyanine. *Energies* **2020**, *13*, 962. [CrossRef]
126. Mdluli, S.B.; Ramoroka, M.E.; Yussuf, S.T.; Modibane, K.D.; John-Denk, V.S.; Iwuoha, E.I. π-Conjugated polymers and their application in organic and hybrid organic-silicon solar cells. *Polymers* **2022**, *14*, 716. [CrossRef]
127. Alahmadi, A.N. Design of an efficient PTB7: PC70BM-based polymer solar cell for 8% efficiency. *Polymers* **2022**, *14*, 889. [CrossRef]
128. Tavasli, A.; Gurunlu, B.; Gunturkun, D.; Isci, R.; Faraji, S. A Review on Solution-Processed Organic Phototransistors and Their Recent Developments. *Electronics* **2022**, *11*, 316. [CrossRef]
129. Zhu, D.; Ji, D.; Li, L.; Hu, W. Recent progress in polymer-based infrared photodetectors. *J. Mater. Chem. C* **2022**, *10*, 13312–13323. [CrossRef]
130. Park, H.-L.; Kim, M.-H.; Kim, H. Enhanced Optical Switching Characteristics of Organic Phototransistor by Adopting Photo-Responsive Polymer in Hybrid Gate-Insulator Configuration. *Polymers* **2020**, *12*, 527. [CrossRef]
131. Kim, T.; Lee, C.; Kim, Y. Near-infrared organic phototransistors with polymeric channel/dielectric/sensing triple layers. *Micromachines* **2020**, *11*, 1061. [CrossRef] [PubMed]
132. Park, H.-L.; Kim, M.-H.; Kim, H. Improvement of photoresponse in organic phototransistors through bulk effect of photoresponsive gate insulators. *Materials* **2020**, *13*, 1565. [CrossRef]
133. Wang, C.-J.; You, H.-C.; Ou, J.-H.; Chu, Y.-Y.; Ko, F.-H. Ultraviolet photodetecting and plasmon-to-electric conversion of controlled inkjet-printing thin-film transistors. *Nanomaterials* **2020**, *10*, 458. [CrossRef]
134. Moschetto, S.; Squeo, B.M.; Reginato, F.; Prosa, M.; Pasini, M.; Toffanin, S. A Fluorescent Conjugated Polar Polymer for Probing Charge Injection in Multilayer Organic Light-Emitting Transistors. *Molecules* **2024**, *29*, 3295. [CrossRef]
135. Gao, W.; Qi, F.; Peng, Z.; Lin, F.R.; Jiang, K.; Zhong, C.; Kaminsky, W.; Guan, Z.; Lee, C.; Marks, T.J.; et al. Achieving 19% power conversion efficiency in planar-mixed heterojunction organic solar cells using a pseudosymmetric electron acceptor. *Adv. Mater.* **2022**, *34*, 2202089. [CrossRef] [PubMed]
136. Wu, C.-C.; Chen, C.-W.; Lin, C.-L.; Yang, C.-J. Advanced organic light-emitting devices for enhancing display performances. *J. Disp. Technol.* **2005**, *1*, 248–266. [CrossRef]
137. Wang, J.; Liu, B. Electronic and optoelectronic applications of solution-processed two-dimensional materials. *Sci. Technol. Adv. Mater.* **2019**, *20*, 992–1009. [CrossRef]
138. Abbel, R.; Galagan, Y.; Groen, P. Roll-to-roll fabrication of solution processed electronics. *Adv. Eng. Mater.* **2018**, *20*, 1701190. [CrossRef]
139. Li, H.; Zuo, C.; Scully, A.D.; Angmo, D.; Yang, J.; Gao, M. Recent progress towards roll-to-roll manufacturing of perovskite solar cells using slot-die processing. *Flex. Print. Electron.* **2020**, *5*, 014006. [CrossRef]
140. Mariotti, N.; Bonomo, M.; Fagiolari, L.; Barbero, N.; Gerbaldi, C.; Bella, F.; Barolo, C. Recent advances in eco-friendly and cost-effective materials towards sustainable dye-sensitized solar cells. *Green Chem.* **2020**, *22*, 7168–7218. [CrossRef]
141. Gundepudi, K.; Neelamraju, P.M.; Sangaraju, S.; Dalapati, G.K.; Ball, W.B.; Ghosh, S.; Chakrabortty, S. A review on the role of nanotechnology in the development of near-infrared photodetectors: Materials, performance metrics, and potential applications. *J. Mater. Sci.* **2023**, *58*, 13889–13924. [CrossRef]
142. Xu, H.; Li, J.; Leung, B.H.K.; Poon, C.C.Y.; Ong, B.S.; Zhang, Y.; Zhao, N. A high-sensitivity near-infrared phototransistor based on an organic bulk heterojunction. *Nanoscale* **2013**, *5*, 11850–11855. [CrossRef] [PubMed]
143. Cao, H.; He, W.; Mao, Y.; Lin, X.; Ishikawa, K.; Dickerson, J.H.; Hess, W.P. Recent progress in degradation and stabilization of organic solar cells. *J. Power Sources* **2014**, *264*, 168–183. [CrossRef]

144. Scholz, S.; Kondakov, D.; Lüssem, B.; Leo, K. Degradation Mechanisms and Reactions in Organic Light-Emitting Devices. *Chem. Rev.* **2015**, *115*, 8449–8503. [CrossRef]
145. Liguori, R.; Nunziata, F.; Aprano, S.; Maglione, M.G. Overcoming Challenges in OLED Technology for Lighting Solutions. *Electronics* **2024**, *13*, 1299. [CrossRef]
146. Park, S.; Kim, T.; Yoon, S.; Koh, C.W.; Woo, H.Y.; Son, H.J. Progress in Materials, Solution Processes, and Long-Term Stability for Large-Area Organic Photovoltaics. *Adv. Mater.* **2020**, *32*, 2002217. [CrossRef]